
Masters Theses

Student Theses and Dissertations

1964

An investigation of the sensitized fluorescence of the mercury-sodium and the cesium-rubidium systems.

Joseph Edward Hueser

Follow this and additional works at: https://scholarsmine.mst.edu/masters_theses



Part of the [Physics Commons](#)

Department:

Recommended Citation

Hueser, Joseph Edward, "An investigation of the sensitized fluorescence of the mercury-sodium and the cesium-rubidium systems." (1964). *Masters Theses*. 5605.

https://scholarsmine.mst.edu/masters_theses/5605

This thesis is brought to you by Scholars' Mine, a service of the Missouri S&T Library and Learning Resources. This work is protected by U. S. Copyright Law. Unauthorized use including reproduction for redistribution requires the permission of the copyright holder. For more information, please contact scholarsmine@mst.edu.

AN INVESTIGATION OF THE SENSITIZED FLUORESCENCE OF THE
MERCURY-SODIUM AND THE CESIUM-RUBIDIUM SYSTEMS

BY

JOSEPH EDWARD HUESER

A

THESIS

submitted to the faculty of the
SCHOOL OF MINES AND METALLURGY OF THE UNIVERSITY OF MISSOURI
in partial fulfillment of the requirements for the

Degree of

MASTER OF SCIENCE, PHYSICS MAJOR

Rolla, Missouri

1964

Approved by

Charles E. Antle (Advisor)

Charles E. Antle

James L. Keesner

Ralph E. Lee

ABSTRACT

The experimental apparatus and techniques used for the study of sensitized fluorescence are discussed. In this study both glass and metal absorption cells were employed. Included also is a discussion of the transitions which occur in the mercury-sodium and the cesium-rubidium systems, which were the two systems investigated. Both photographic and photometric techniques were used as means of detecting the sensitized fluorescence. The actual experimental apparatus used are discussed together with conclusions to be drawn and recommendations to be made from the individual experiments. The purpose of the experiments was to better understand the energy exchange processes in a two element system. Conclusions and recommendations are made mainly for the cesium-rubidium system and although no quantitative data was obtained, sufficient recommendations are made so that an extensive, quantitative study of the sensitized fluorescence of the cesium-rubidium system could be performed.

ACKNOWLEDGMENTS

The author wishes to express his gratitude to those who gave assistance and guidance in this project, especially Dr. Richard Anderson, whose guidance in the capacity of advisor made the project possible.

An expression of gratitude goes also to those at the McDonnell Aircraft Corporation laboratories who made it possible to expedite the experimental investigation by the use of their facilities.

TABLE OF CONTENTS

	Page
ABSTRACT	11
ACKNOWLEDGMENTS	111
LIST OF FIGURES	v
LIST OF TABLES	vii
I. INTRODUCTION	1
General Theory	1
Sensitized Fluorescence	8
II. REVIEW OF LITERATURE	10
Mercury-Sodium System	10
Statement of Mercury-Sodium Problem	12
Cesium-Rubidium System	15
Statement of Cesium-Rubidium Problem	16
III. EXPERIMENTAL TECHNIQUES	20
Cell Fabrication	20
Spectrographic Studies	20
Electron Multiplier Techniques	24
IV. EXPERIMENTAL APPARATUS	27
Initial Apparatus	27
Final Apparatus	36
V. DISCUSSION OF RESULTS AND CONCLUSIONS	64
BIBLIOGRAPHY	66
VITA	67

LIST OF FIGURES

Figure	Page
1. Mercury energy level diagram	3
2. Illustration of sensitized fluorescence	9
3. Sodium energy level diagram	11
4. Cesium energy level diagram	17
5. Rubidium energy level diagram	18
6. Typical characteristic curve.	23
7. Block diagram of the photometric detection system	26
8. Quartz absorption cell.	28
9. Monochromator used in the initial test.	29
10. Initial glass vacuum system	30
11. Cell, oven, and distillation units.	32
12. Initial photometric detection system.	33
13. All metal vacuum system	38
14. Completed metal cell.	39
15. Rear section of metal cell.	40
16. Front section of metal cell	41
17. Vapor pressure curve for cesium	47
18. Vapor pressure curve for rubidium	48
19. Pyrex cylindrical cell.	50
20. Side view of oven and light source.	51
21. Front view of oven showing cell mounting.	52
22. Side view of corroded pyrex cell.	54
23. Front view of corroded pyrex cell	55

Figure	Page
24. Top view of final test apparatus.	57
25. Front view of final test apparatus.	58
26. Side view of final test apparatus	59
27. Side view of Corning 7280 glass cell.	61
28. Front view of Corning 7280 glass cell	62

LIST OF TABLES

Table	Page
I. Photographic plate I-3 of sensitized fluorescence	43
II. Photographic plate I-4 of sensitized fluorescence	44
III. Photographic plate I-5 of sensitized fluorescence	45
IV. Photographic plate I-6 of sensitized fluorescence	46

I. INTRODUCTION

General Theory

According to the postulates of the Bohr theory, the energy of a system can increase only in discrete steps; therefore, the system exists in discrete yet well defined stationary energy states. If one applies these considerations to the atom, there exist discrete energy levels and the lowest is called the ground level or ground state of the atom. Furthermore, the Bohr theory employed the following relation for a transition between two energy levels E and E' : $(E' - E) = h\nu$, where h is Planck's constant (6.62×10^{-27} erg sec) and ν is the frequency of the radiation which is absorbed or emitted in the transition.

Bohr adopted the Rutherford model of the atom which consisted of a nucleus surrounded by electrons, which were later found to be contained in definite shells and subshells. The shell or orbit in which the electron exists dictates the integral value of n . The quantum number ℓ represents the orbital angular momentum of the electron measured in units of $h/2\pi$ and can assume integral values from 0 to $n-1$. Adopting the spectroscopic notation, the values of ℓ are represented by letters as follows:

	S	P	D	F	G	.	.	.
ℓ	= 0	1	2	3	4	.	.	.

The observed multiple energy states of the emission

spectra are explained by the spin of the electron which is expressed in units of $h/2\pi$. The spin quantum number s is an inherent property of the electron and can have values of $\pm 1/2$. The total angular momentum j is the vector sum of ℓ and s . Each of the quantum numbers ℓ , s , and j of the individual electrons has a counterpart L , S , and J which is the vector sum of all ℓ , all s , or all j of the valence electrons of that particular atom. These quantum numbers together with the multiplicity are all that are needed to define an energy state.

In order to illustrate the energy levels which exist for a given atom, it is customary to use an energy level diagram. Each term or energy level is represented by its respective quantum numbers n , ℓ , and s , where n is the principal quantum number, ℓ is the orbital angular momentum quantum number, and s is the spin angular momentum quantum number. A typical example is the 6^3P_1 (six triplet P one) state of mercury shown in Figure 1. The quantum number n appears first (in this case, 6) and represents an electron in the sixth shell. The superscript 3 indicates that the state is a triplet. The letter P gives the quantum number L , which in this case is one. The subscript 1 is the quantum number J , which in this case is the vector sum of $L = 1$ and $S = 1$ to give $J = 1$. The mercury atom has two valence electrons; the rest of the electrons are more tightly bound to the nucleus either in closed shells or

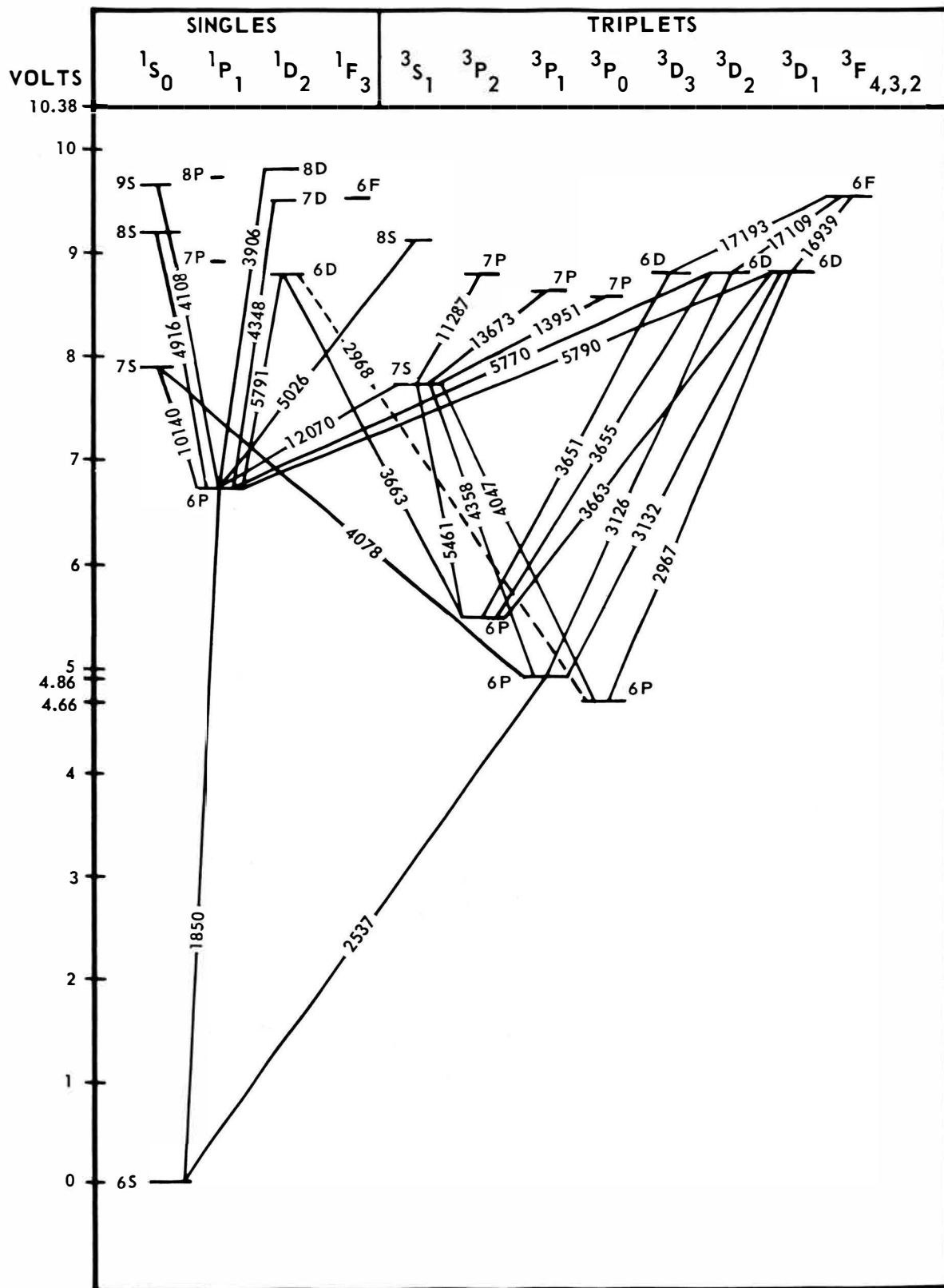


FIGURE 1
MERCURY ENERGY LEVEL DIAGRAM

closed subshells. The 6P level of mercury has a singlet and a triplet state. If the two electron spins are antiparallel, $S = 0$, the energy level is a singlet since the only possible value for J is 1. On the other hand, if the electron spins are parallel, $S = 1$ and the energy level is a triplet since J can have the values 2, 1, or 0. Also appearing in any energy level diagram is the relative separation between the energy states which is given either in electron volts or wave numbers. Also the wavelength of the emitted radiation corresponding to the transition from the higher to the lower energy state is given.

Since all possible transitions do not occur, a set of selection rules have been determined based on the transition probabilities between specific energy levels. The selection rules for electric dipole radiation are as follows:

1. $\Delta L = \pm 1$
2. $\Delta J = \pm 1$ or 0, excluding $J = 0 \rightarrow J = 0$.

These selection rules are based on experimental observations and theory. They give the allowed transitions with probabilities which are high enough so that the emission spectra can be observed using ordinary spectrographic techniques with moderate resolving power.

The former considerations include only conclusions which can be derived by employing quantum mechanics and have neglected the hyperfine structure which can be explained by nuclear spin.

The fact that certain transitions have been observed which violate the selection rules indicates that this explanation is far from complete; however, it does serve our purpose.

There is a glow associated with arc, spark, and flame sources. These glows are typical examples of the emission spectra characteristic of atoms or molecules and represent the transition of an atom or molecule from a higher to a lower energy state. The process is called luminescence, a generic term representing the emission of radiation at some characteristic frequency caused by excitation to a higher energy state. A particular type of luminescence is photoluminescence which is the emission of radiation caused by light excitation.

For a one element system, the radiation emitted is either fluorescence or phosphorescence. Early investigators made a distinction between fluorescence and phosphorescence by the length of time that the afterglow existed after the exciting light was removed. If the luminescence lasted only as long as the irradiation, it was called fluorescence; if it remained after the exciting light was shut off, it was called phosphorescence. If one irradiates a one element system with monochromatic radiation of frequency ν , there may be observed the emission of radiation of frequencies other than ν . This type of luminescence is called fluorescence and the lifetime of the excited states is usually

of the order of 10^{-7} or 10^{-8} sec. If the only frequency observed is the same as the irradiation frequency, the fluorescence is called resonance radiation.

Referring to Figure 1, page 3, it is noticed that there is no transition wavelength between the 6^3P_0 state and the 6^1S_0 ground state. The 6^3P_0 state and similar states which are prohibited by the selection rules from making transitions to a lower energy state and emitting their characteristic wavelength are called metastable states. Because of the low transition probability between the metastable states and lower energy states, their lifetime is longer. Metastable atoms may have their theoretical lifetime shortened by three processes:

1. They may collide with other atoms and be excited to a level from which transitions are allowed.
2. They may suffer nonradiative collisions with other atoms and their excitation energy be transferred to the other atom.
3. They may suffer collisions with the nearly infinite walls of the container with a loss of their energy and angular momentum.

If a cell containing mercury vapor is irradiated with $2537\overset{\circ}{\text{A}}$ light, atoms are excited from the 6^1S_0 state to the 6^3P_1 state. Emission of the $2537\overset{\circ}{\text{A}}$ line as the atom returns to the ground state is an example of resonance radiation. However, some of the atoms in the 6^3P_1 state can be trans-

ferred into the 6^3P_0 metastable state by colliding with other atoms. If the exciting light is turned off, one observes that the $2537\overset{\circ}{\text{A}}$ radiation is still present after a relatively long time. This phenomena cannot be explained by the resonance radiation because of its short lifetime. Here the 6^3P_0 atoms are acquiring sufficient energy by collisions to return to the 6^3P_1 state and these atoms are returning to the ground state by the emission of the $2537\overset{\circ}{\text{A}}$ line. This process, involving a metastable state, is called phosphorescence. With the proper experimental conditions, the emission of the forbidden line $2665\overset{\circ}{\text{A}}$ ($6^3P_0 \rightarrow 6^1S_0$) can be observed. Since the transition probability is low, the lifetime of the 6^3P_0 state is long. This type of luminescence is called fluorescence of long duration. One can see then that the length of time that the afterglow exists does not determine whether the luminescence is fluorescence or phosphorescence but that the type of transitions involved is the determining factor.

Frank and Hertz discovered in 1913 that an electron with sufficient kinetic energy can collide with a normal atom producing a slow electron and an excited atom; this process has been termed a collision of the first kind. Klein and Rosseland¹, employing the principle of microscopic reversability, reasoned that the inverse process should occur; namely, an excited atom upon colliding with a slow electron can produce a fast electron and a normal atom.

This process is called a collision of the second kind. Frank extended this idea to include collisions between two atoms or molecules. He reasoned that an excited atom could collide with a normal atom resulting in an exchange of energy. The normal atom would receive the energy as kinetic energy, excitational energy, or both.

Sensitized Fluorescence

Consider a cell containing two species of atoms A and B. For the purpose of illustration, consider only the ground state and one excited level of each species. The energy level diagrams would then appear as in Figure 2.

By the absorption of energy of frequency ν , atoms A are raised to the excited state. If the lifetime of this excited state is of the same order of magnitude as the collision frequency between atoms A and B, there will be produced, by collisions of the second kind, normal atoms A and excited atoms B. Both frequencies ν and ν' will then appear. This process of energy exchange is known as sensitized fluorescence and is the process of principal interest. The two excited states are said to be in energy resonance if ΔE is zero. The probability of the energy transfer taking place by a collision of the second kind increases as ΔE becomes smaller. By the conservation of energy and momentum, one can calculate the relative velocities of the atoms A and B before and after the collision.

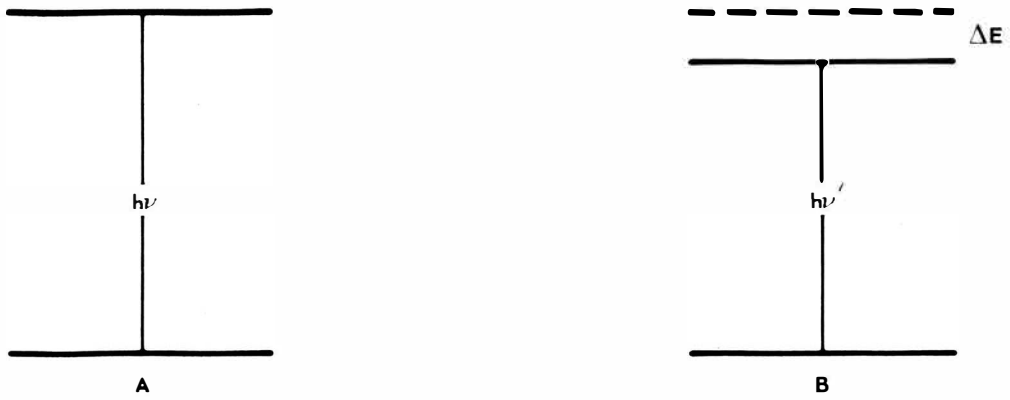


FIGURE 2
ILLUSTRATION OF SENSITIZED FLUORESCENCE

II. REVIEW OF LITERATURE

Mercury-Sodium System

In an attempt to verify the theory that the probability for energy exchange increases as ΔE decreases, Beutler and Josephy² studied the sensitized fluorescence spectra of a mercury-sodium system. Figure 1, page 3, shows the energy level diagram for mercury and Figure 3 shows the energy level diagram for sodium. Assuming equal transition probabilities, one would expect that the intensity of sodium lines arising from transitions of higher n values would decrease since the excitation energy increases. However, Beutler and Josephy showed that this was not the case. In fact, they found in the series $n^2S \rightarrow 3^2P$ that the lines arising from the $9^2S \rightarrow 3^2P$ transitions were by far the most intense. The reason was that the 9^2S level is in near resonance with the 6^3P_1 state of mercury. The 8^2P state of sodium would probably produce more intense lines, but they could not resolve these wavelengths because they were too close to the resonance line of mercury. There was also an enhancement of the $7^2S \rightarrow 3^2P$ transitions since the 7^2S state is in near energy resonance with the 6^3P_0 state of mercury. These two instances support the theory that the probability of energy transfer increases as the energy difference decreases.

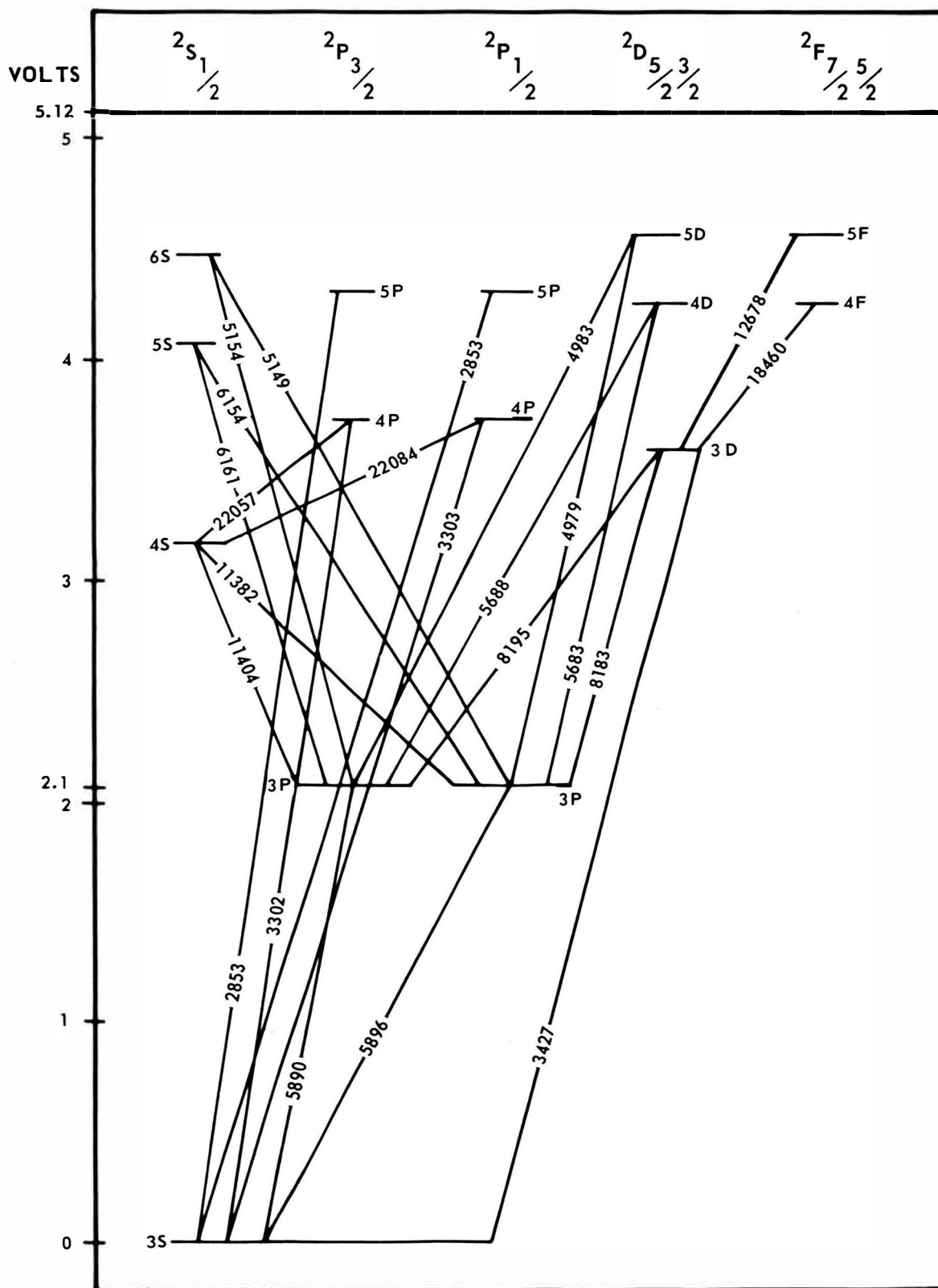


FIGURE 3
SODIUM ENERGY LEVEL DIAGRAM

Statement of the Mercury-Sodium Problem

The general objective of the initial experiment was to further investigate the energy exchange in the mercury-sodium system. The main aim of the experiment was to establish the temperature dependence of the sensitized fluorescence. This experiment consisted of varying the mercury and sodium vapor pressures independently and the sodium line intensities of known transitions would be plotted versus sodium and mercury temperatures.

The purpose of the experiment was threefold:

1. to support the work done by Swanson and McFarland³, who used a mercury-thallium system, by showing that the same conclusions could be drawn using a different system;
2. to try to better explain and understand the energy exchange processes of normally excited mercury atoms, metastable mercury atoms, and mercury molecules with unexcited atoms of another species and also to investigate the quasi-molecules formed by the two species in the cell;
3. to determine the lifetimes of the excited sodium states by performing decay studies of both direct and cascade transitions.

Swanson and McFarland based their conclusions on the validity of Winan's partial selection rule⁴, which makes the assumption that the two atoms form a quasi-molecule in

the collision. The assumptions made are verified by experimental results and for the cases cited proved that the probability of energy transfer increases when the resultant angular momentum of the quasi-molecule does not change in the collision. This gives the selection rule $\Delta J = 0$, where J is the resultant angular momentum of the quasi-molecule formed by the two atoms.

Mercury was a natural choice for one of the elements because it is readily available, it is easy to use, and an enormous amount of information is available concerning its physical properties and behavior. Mercury light sources were also readily available. Sodium was picked as the second element because it is also inexpensive, readily available, and relatively easy to use; but, most important, there are a large number of sodium energy levels which have small energy differences with the 6^3P_1 and 6^3P_0 mercury atomic states and the metastable mercury molecules. In addition, the elements selected had to have a sufficiently high vapor pressure, around 1mm of mercury, at temperatures which are compatible with materials commonly used for fabrication of the cells, usually pyrex or quartz.

The transitions to be studied were picked because of the demands of the detection system to be employed. The transitions were as follows:

1. $10^2S_{1/2} \longrightarrow 3^2P_{1/2}$ (4343 $\overset{\circ}{\text{A}}$)
2. $10^2S_{1/2} \longrightarrow 3^2P_{3/2}$ (4346 $\overset{\circ}{\text{A}}$)

3.	$9^2S_{1/2} \longrightarrow 3^2P_{1/2}$	(4421 $\overset{\circ}{\text{Å}}$)
4.	$9^2S_{1/2} \longrightarrow 3^2P_{3/2}$	(4424 $\overset{\circ}{\text{Å}}$)
5.	$8^2S_{1/2} \longrightarrow 3^2P_{1/2}$	(4543 $\overset{\circ}{\text{Å}}$)
6.	$8^2S_{1/2} \longrightarrow 3^2P_{3/2}$	(4546 $\overset{\circ}{\text{Å}}$)
7.	$7^2S_{1/2} \longrightarrow 3^2P_{1/2}$	(4750 $\overset{\circ}{\text{Å}}$)
8.	$7^2S_{1/2} \longrightarrow 3^2P_{3/2}$	(4754 $\overset{\circ}{\text{Å}}$)
9.	$6^2S_{1/2} \longrightarrow 3^2P_{1/2}$	(5149 $\overset{\circ}{\text{Å}}$)
10.	$6^2S_{1/2} \longrightarrow 3^2P_{3/2}$	(5154 $\overset{\circ}{\text{Å}}$)
11.	$5^2S_{1/2} \longrightarrow 3^2P_{1/2}$	(6154 $\overset{\circ}{\text{Å}}$)
12.	$5^2S_{1/2} \longrightarrow 3^2P_{3/2}$	(6161 $\overset{\circ}{\text{Å}}$)
13.	$9^2P_{3/2, 1/2} \longrightarrow 3^2S_{1/2}$	(2513 $\overset{\circ}{\text{Å}}$)
14.	$8^2P_{3/2, 1/2} \longrightarrow 3^2S_{1/2}$	(2545 $\overset{\circ}{\text{Å}}$)
15.	$7^2P_{3/2, 1/2} \longrightarrow 3^2S_{1/2}$	(2595 $\overset{\circ}{\text{Å}}$)
16.	$6^2P_{3/2, 1/2} \longrightarrow 3^2S_{1/2}$	(2681 $\overset{\circ}{\text{Å}}$)
17.	$5^2P_{3/2, 1/2} \longrightarrow 3^2S_{1/2}$	(2853 $\overset{\circ}{\text{Å}}$)
18.	$9^2D \longrightarrow 3^2P_{1/2}$	(4322 $\overset{\circ}{\text{Å}}$)
19.	$9^2D \longrightarrow 3^2P_{3/2}$	(4326 $\overset{\circ}{\text{Å}}$)
20.	$8^2D \longrightarrow 3^2P_{1/2}$	(4391 $\overset{\circ}{\text{Å}}$)
21.	$8^2D \longrightarrow 3^2P_{3/2}$	(4395 $\overset{\circ}{\text{Å}}$)
22.	$7^2D \longrightarrow 3^2P_{1/2}$	(4496 $\overset{\circ}{\text{Å}}$)
23.	$7^2D \longrightarrow 3^2P_{3/2}$	(4499 $\overset{\circ}{\text{Å}}$)
24.	$6^2D \longrightarrow 3^2P_{1/2}$	(4666 $\overset{\circ}{\text{Å}}$)
25.	$6^2D \longrightarrow 3^2P_{3/2}$	(4670 $\overset{\circ}{\text{Å}}$)
26.	$5^2D \longrightarrow 3^2P_{1/2}$	(4979 $\overset{\circ}{\text{Å}}$)
27.	$5^2D \longrightarrow 3^2P_{3/2}$	(4983 $\overset{\circ}{\text{Å}}$)

$$28. \quad 4^2D \longrightarrow 3^2P_{1/2} \quad (5683\overset{\circ}{\text{A}})$$

$$29. \quad 4^2D \longrightarrow 3^2P_{3/2} \quad (5688\overset{\circ}{\text{A}})$$

It is probable that most of these doublets would not be resolved by the monochromator and would have to be read together. Also, some of the transition wavelengths would not be resolved because of close mercury lines.

Cesium-Rubidium System

Little information was available in the literature concerning the cesium-rubidium system. There have been no experiments performed on the sensitized fluorescence of the cesium-rubidium system. Therefore, all the insight into the problem had to be drawn from the general properties of sensitized fluorescence and from similarities to other systems.

Early experiments by Boeckner⁵ and Mohler and Boeckner⁶ on the quenching of the resonance radiation of cesium vapor and later experiments by Jacobs et al.⁷ and Cummins et al.⁸ on optical pumping of cesium vapor showed that the $8^2P_{1/2}$ cesium state corresponding to a resonance transition of $3888\overset{\circ}{\text{A}}$ is effectively excited by the strong $3888\overset{\circ}{\text{A}}$ helium line. This should be expected since the two wavelengths differ by only $0.037\overset{\circ}{\text{A}}$. Therefore, it was decided to use a commercially available helium arc as the excitation source for the cesium vapor rather than build a cesium source.

Statement of the Cesium-Rubidium Problem

The final part of this investigation was essentially the same as the first: to study the mechanism of energy exchange within a two element system. Cesium was chosen as a first element because it possesses physical properties which are necessary in the study of fluorescence: it has an experimentally feasible vapor pressure at low temperatures; it has low energy excited states; and it can be excited to the $8^2P_{1/2}$ state by readily available helium lamps. Rubidium was picked as the second element because it possesses excited energy states with small energy differences to the excited cesium state.

The majority of the wavelengths corresponding to the transitions of interest are in the near infra-red region, between 7000\AA and 8000\AA . Neither the school nor our laboratory possessed an electron multiplier which was sensitive in this region, so a spectrograph and type I-N photographic plates were used for detection.

Figures 4 and 5 show the energy level diagrams of cesium and rubidium, respectively. The expected sequence of events leading to the observance of the sensitized fluorescence was as follows: the helium source would excite the cesium vapor to the $8^2P_{1/2}$ state; then by collisions of the second kind, the excitation energy would be transferred to the normal rubidium atoms, which would decay to the ground state emitting their characteristic frequencies.

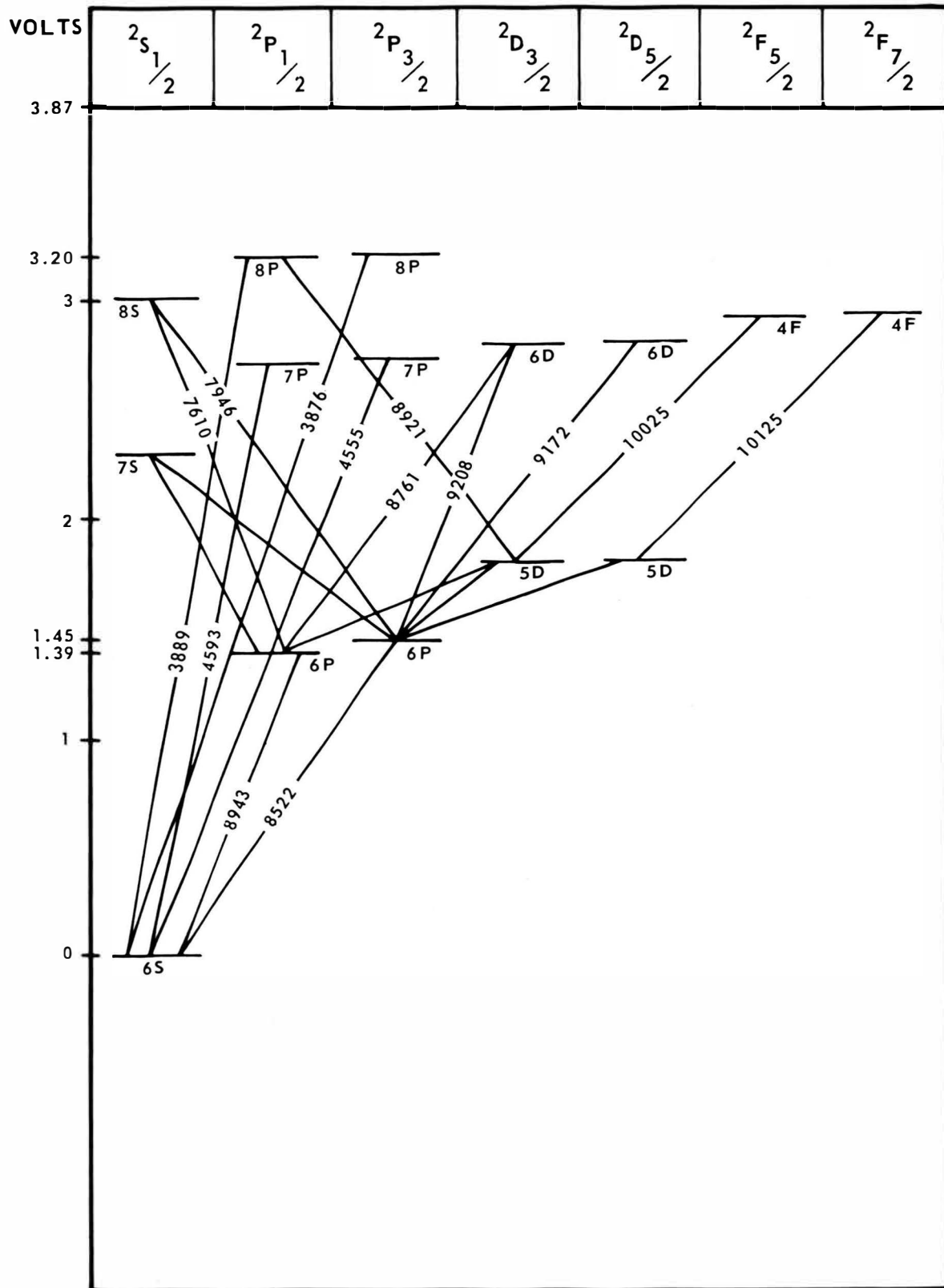


FIGURE 4
CESIUM ENERGY LEVEL DIAGRAM

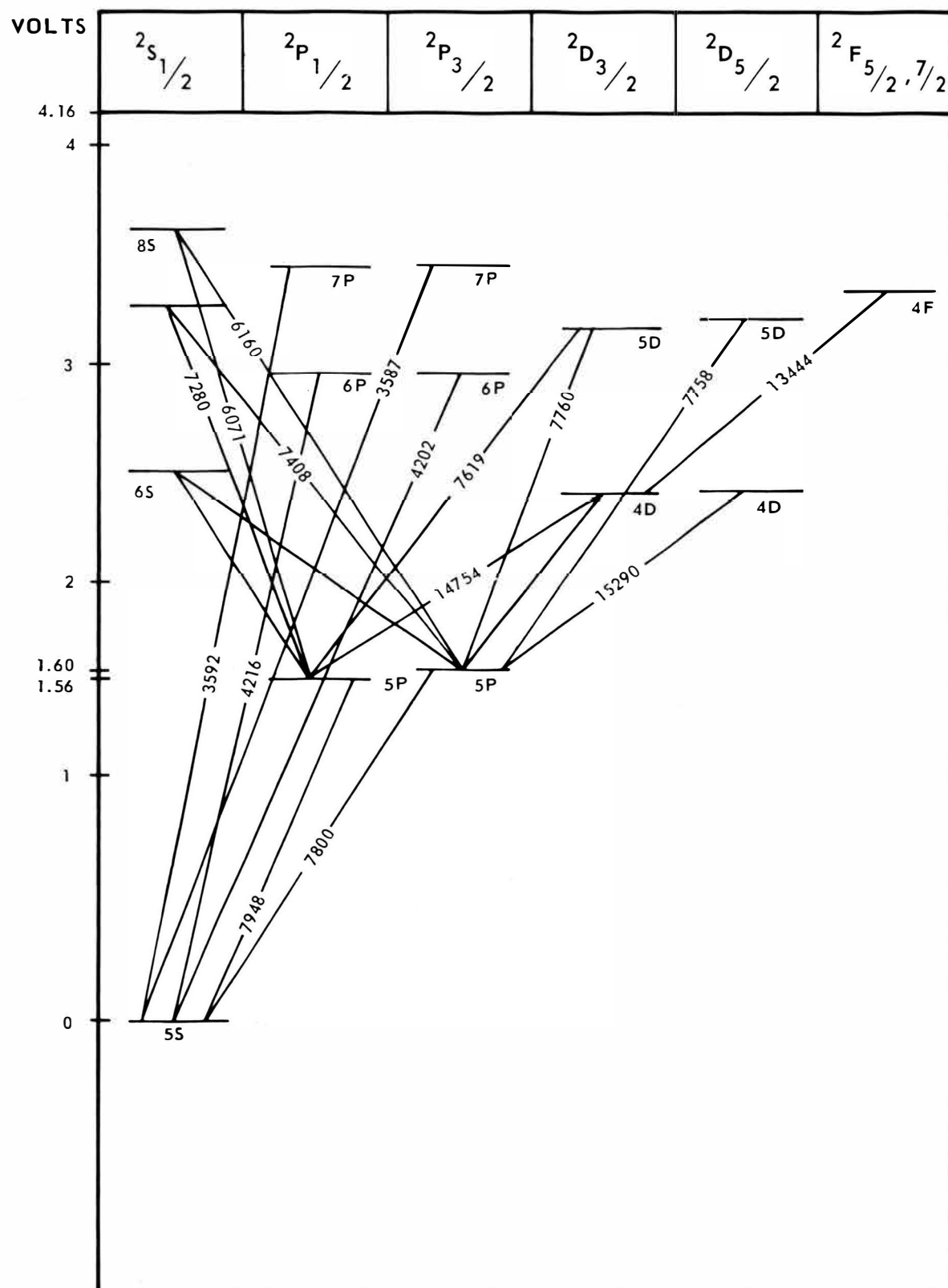


FIGURE 5

RUBIDIUM ENERGY LEVEL DIAGRAM

Using the criterion that the lines corresponding to the smallest energy difference are the most intense, the investigated transitions are listed below in the order of decreasing intensity:

1. $5^2D_{3/2} \rightarrow 5^2P_{3/2}$ (7760 $\overset{\circ}{\text{A}}$)
2. $5^2D_{3/2} \rightarrow 5^2P_{1/2}$ (7619 $\overset{\circ}{\text{A}}$)
3. $5^2D_{5/2} \rightarrow 5^2P_{3/2}$ (7758 $\overset{\circ}{\text{A}}$)
4. $7^2S_{1/2} \rightarrow 5^2P_{3/2}$ (7408 $\overset{\circ}{\text{A}}$)
5. $7^2S_{1/2} \rightarrow 5^2P_{1/2}$ (7280 $\overset{\circ}{\text{A}}$)
6. $6^2P_{3/2} \rightarrow 5^2S_{1/2}$ (4202 $\overset{\circ}{\text{A}}$)
7. $6^2P_{1/2} \rightarrow 5^2S_{1/2}$ (4216 $\overset{\circ}{\text{A}}$)
8. $7^2P_{3/2} \rightarrow 5^2S_{1/2}$ (3587 $\overset{\circ}{\text{A}}$)
9. $7^2P_{1/2} \rightarrow 5^2S_{1/2}$ (3592 $\overset{\circ}{\text{A}}$)

Since many of the transitions are cascade transitions including the 5^2P levels, the 7948 $\overset{\circ}{\text{A}}$ and 7800 $\overset{\circ}{\text{A}}$ lines should also be predominant lines.

III. EXPERIMENTAL TECHNIQUES

Cell Fabrication

In the first experiment the cells were fabricated of quartz and were made by a professional glass blower at the University of Missouri. The rest of the glass work and the cells used in the later experiments were made by the author. For all end window seals, the tubular section was ground and polished on a metallographic wheel and the windows then sealed to this polished surface. When the window was pyrex, it was fused to the tube with a hand torch using natural gas and oxygen. The entire unit was then oven annealed. When the window was sapphire, it was fused to the Corning 7280 glass using a technique similar to the one described in an article by R. A. Anderson and E. E. Stepp⁹.

In order to break the glass capsules containing the specimens inside the vacuum distillation apparatus and in the all metal cell, an .020 wall stainless steel tube was fabricated into the glass system using a pyrex-to-Kovar graded seal. After the system had been pumped down, the glass capsule was then crushed inside the stainless steel tube with a pair of pliers.

Spectrographic Studies

The spectrograph used for part of the work was a Baird-Atomic three meter grating instrument model GX-1. The grating was a 15,000 lines/inch concave grating. The

linear dispersion in the first order at the camera for the wavelength region in question was over $5.6\text{\AA}/\text{mm}$.

The photographic plates used were class N, type I. Class N was the only choice because it is the only emulsion which is sensitive in the region of interest. The region of sensitivity extends from 6700\AA to 8800\AA . Of the two types that are available, type I and type IV, data only on type I could be found. Type I-N plates are coarse grained, medium contrast with an average resolving power of 82 lines/mm. This limits the theoretical resolving power to 0.07\AA in the region of interest. However, it is not necessary that the detection system be capable of high resolution. In fact, a capability of resolving lines which are 1\AA or 2\AA apart is more than adequate for this type of experiment.

For a complete description of spectrographic apparatus and techniques, refer to Experimental Spectroscopy¹⁰. Chapter 8 of this book is especially useful in understanding the physical properties of the photographic emulsion. In order for a photographic measurement to be meaningful and accurate, one must always bear in mind that there are numerous steps to be taken before the data is in tangible form. For this reason, a definite procedure must be adopted and adhered to in all cases. As the need for accuracy increases, the amount of care and work involved also increases. Since this experiment did not require a high

degree of accuracy, assumptions were made that could not be made in some types of work. The following were the assumptions made:

1. It was assumed that the density of the emulsion support, in this case a glass plate, was uniform.
2. It was assumed that all the plates from a given box, but not necessarily plates taken from different boxes, were processed in the same manner and would be uniform.
3. It was assumed that the response of the emulsion to a particular frequency would be constant across the plate.

The plates were calibrated for spectral sensitivity in the range 6700\AA to 8800\AA , which included all of the expected transitions except the four lines arising from the transitions $6^2P_{3/2, 1/2} \rightarrow 5^2S_{1/2}$ and $7^2P_{3/2, 1/2} \rightarrow 5^2S_{1/2}$. These could have been studied later if the time and necessity arose. The plates were compared against a standard NBS tungsten ribbon filament lamp. The filament temperature was measured with an optical pyrometer and the power density at the desired wavelengths calculated. From these values together with the exposure times and the plate densities, one can plot the characteristic curve, which is also called the H-D curve after Hurter and Driffield. A typical characteristic curve is shown in Figure 6.

Point A on the curve represents the threshold intensity

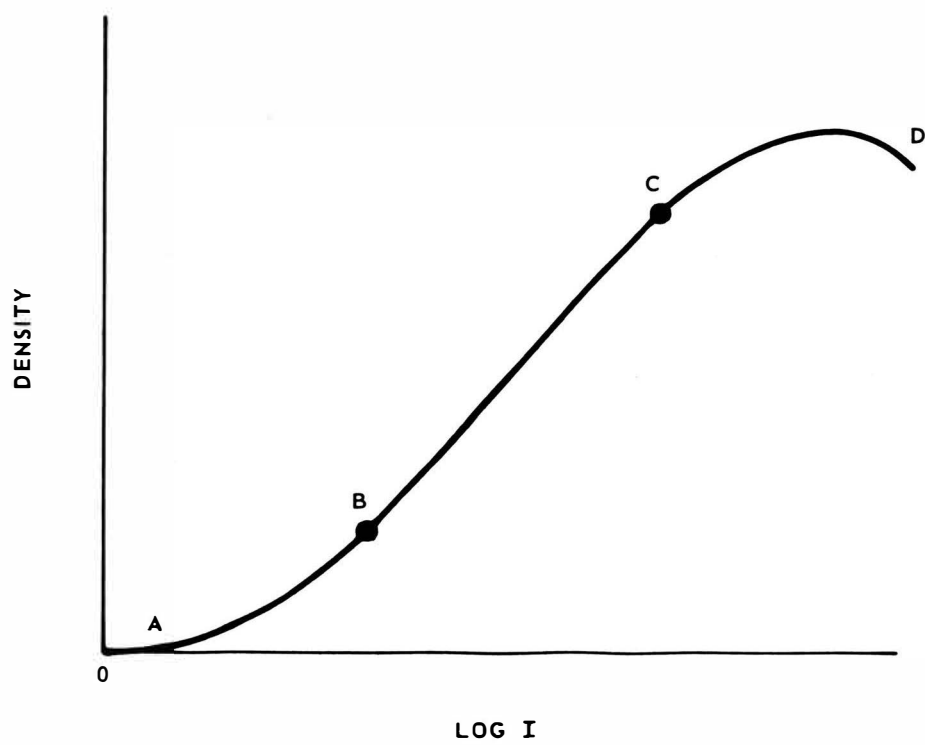


FIGURE 6
TYPICAL CHARACTERISTIC CURVE

at which plate darkening is first measurable. One usually tries to take data so that the density measurements fall in the region BC where the log of the intensity is a linear function of the plate density. The rest of the curve CD represents a region of decreasing response followed by a density reversal.

Once the characteristic curve for a given wavelength has been plotted, one has a means of determining the relative intensities of the spectral lines in question. By knowing the exposure time and the line density, the line intensity can be computed from the experimentally determined characteristic curve.

Electron Multiplier Techniques

Another means of detection employed an electron multiplier with the output amplified and exhibited on a read out device. The photometric detection is not as sensitive as the photographic technique but in some ways it is desirable. The two outstanding advantages are time and effort. The photographic technique provides a permanent record but the amount of time required per data point is at least an order of magnitude higher. The amount of effort required to produce the same quality of data is also higher; for example, cleanliness in procedure and consistency of individual operations such as development of plates.

The photometric detection system consisted of a Bausch

and Lomb model 33-86-45 grating monochromator and an RCA model 7102 electron multiplier. The output of the electron multiplier was fed into a twin-t amplifier tuned to 120 c.p.s. The output of the amplifier was read on an audio voltmeter. Figure 7 is a block diagram of the system used.

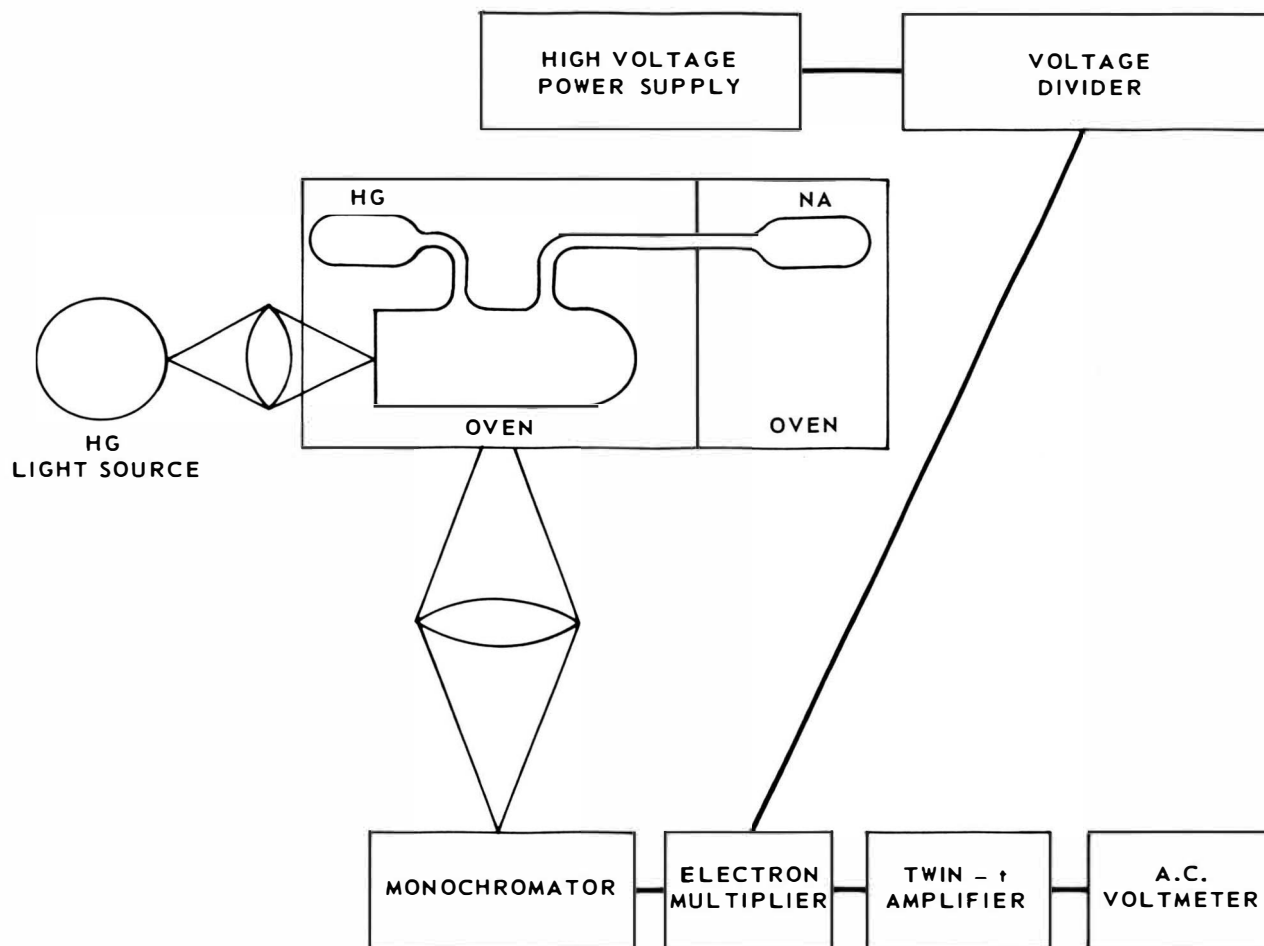


FIGURE 7
BLOCK DIAGRAM OF THE PHOTOMETRIC DETECTION SYSTEM

IV. EXPERIMENTAL APPARATUS

Initial Apparatus

In the period between January, 1959, and June, 1960, the first experimental apparatus was fabricated and the first experiment was run. The test apparatus consisted of the following:

1. vacuum pumping system:
 - A. H. S. Martin three stage mercury diffusion pump with a theoretical pumping speed of 50 liters/sec;
 - B. Welch mechanical pump with a pumping speed of 21 liters/min;
 - C. dry ice and acetone cold traps;
 - D. CVC thermocouple gauge model GTC-100;
 - E. CVC ion gauge model GIC-110;
2. quartz absorption cell (see Figure 8);
3. monochromator designed and built at the Missouri School of Mines and Metallurgy (see Figure 9);
4. 1P28 electron multiplier tube and associated electronics.

A considerable amount of the initial effort was spent in building the equipment to be used for the experiment. The pumping system was fabricated of pyrex glass with a graded seal to quartz in order to attach the absorption cell. Figure 10 shows the completed vacuum system and

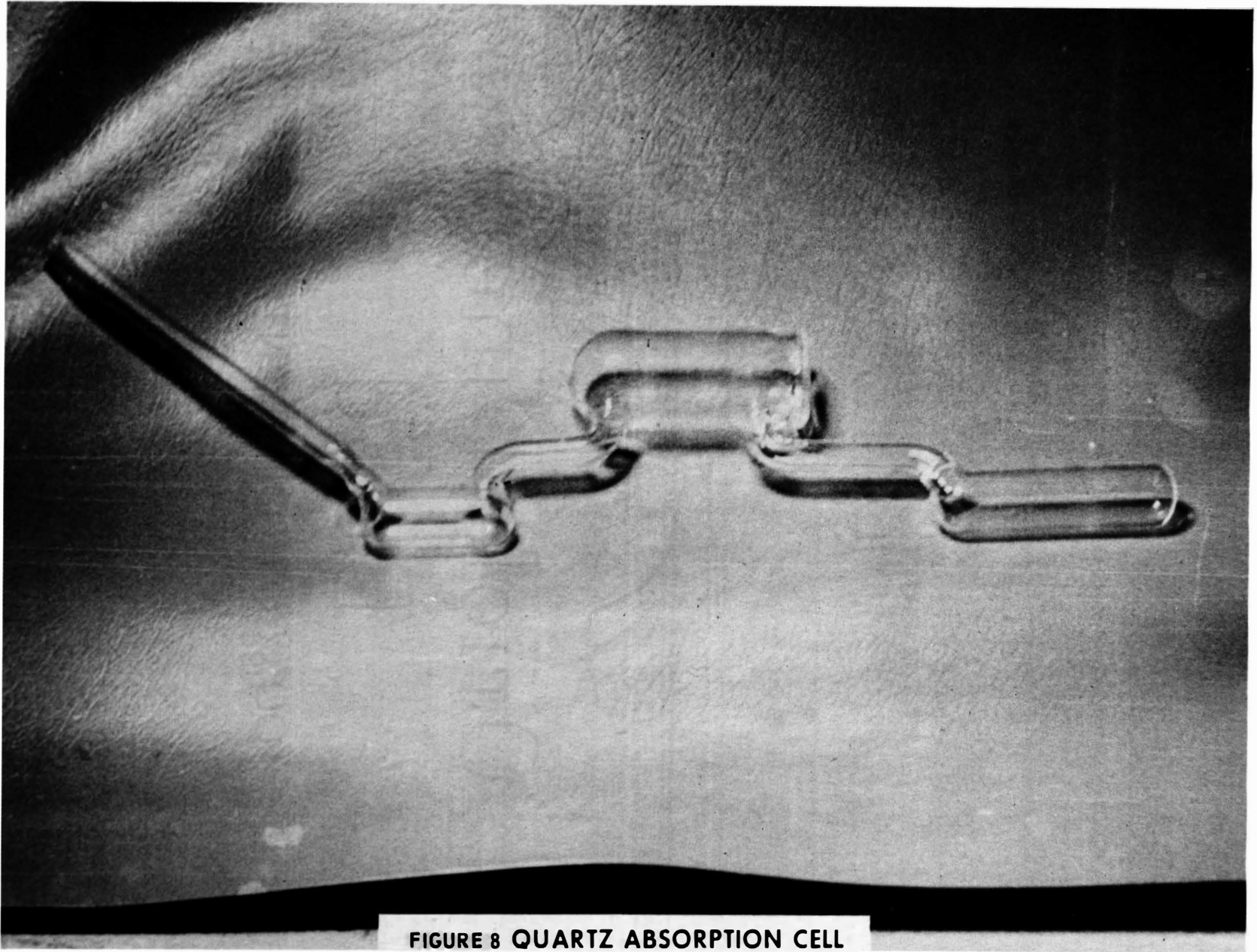


FIGURE 8 QUARTZ ABSORPTION CELL

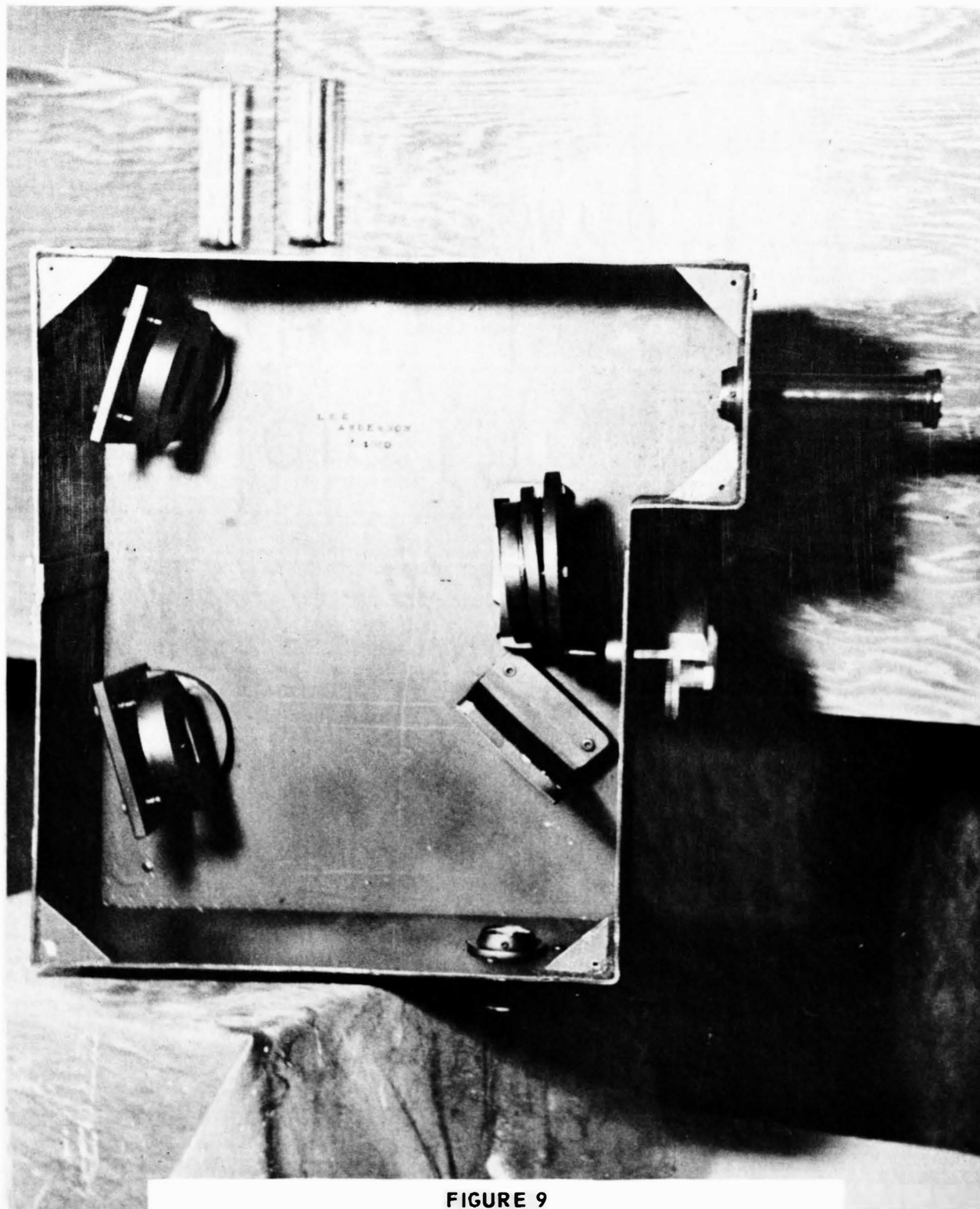


FIGURE 9
MONOCHROMATOR USED IN THE INITIAL TEST

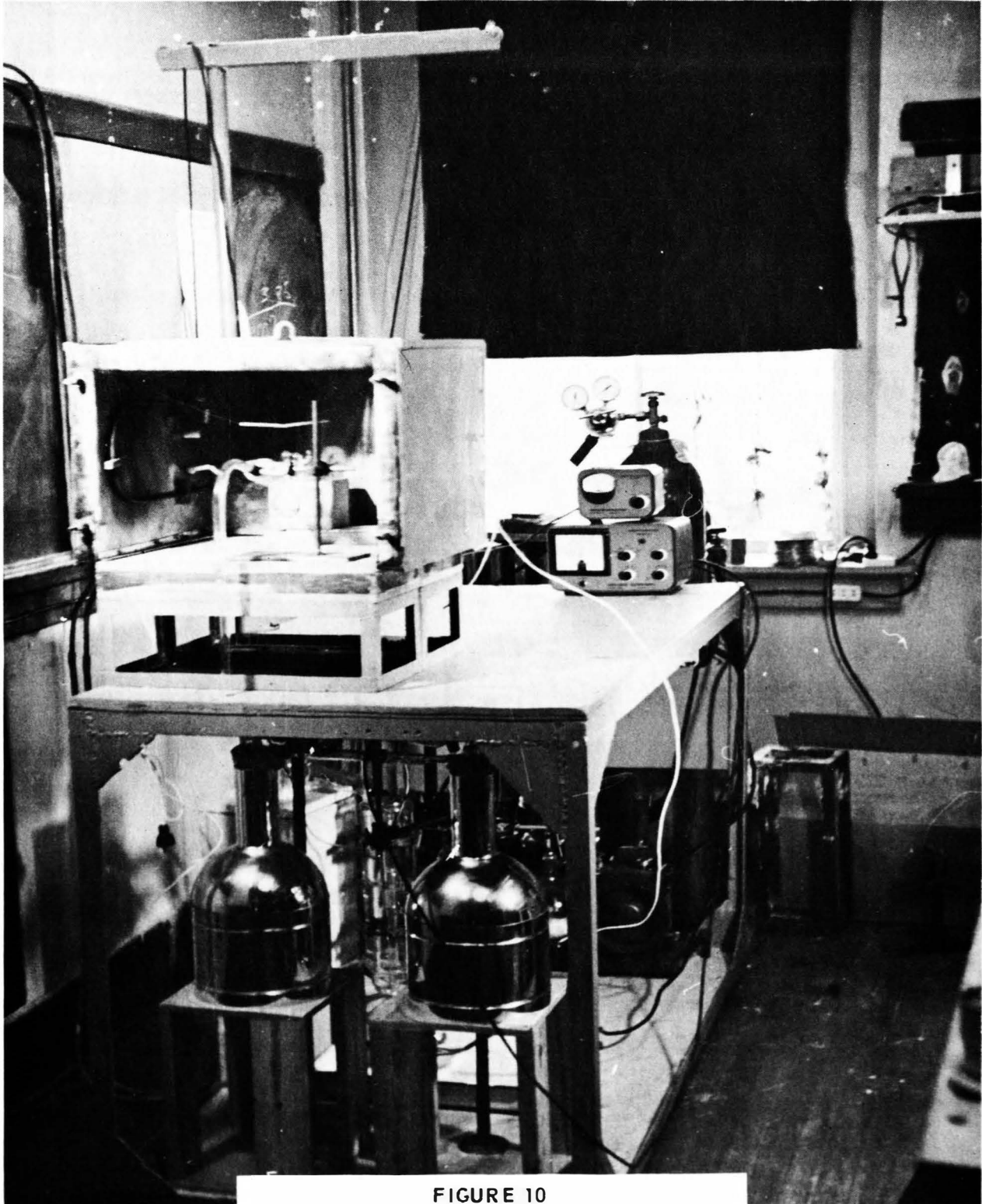


FIGURE 10
INITIAL GLASS VACUUM SYSTEM

bakeout ovens. The mercury distillation unit is inside the main oven. Figure 11 shows the absorption cell mounted in its oven and the sodium distillation unit wrapped with heater wires. Figure 12 shows the completed monochromator with the 1P28 electron multiplier detector mounted at the exit slit. Shown also are the power supply for the electron multiplier and the Keithley electrometer model 200B which was used to read the output signal of the electron multiplier.

The absorption cell for the experiment was prepared as follows:

1. The entire system was pumped down and outgassed and after it had cooled down, the pressure in the system reached 10^{-6} Torr.
2. The system was backfilled with dry nitrogen gas and the mercury and sodium inserted into their respective distillation units.
3. The nitrogen was then pumped out of the system.
4. The sodium was triply distilled into its reservoir and the distillation unit sealed off at the reservoir.
5. The mercury was doubly distilled into its reservoir and the absorption cell sealed off and removed from the vacuum system.
6. The absorption cell was mounted in the main part of the oven, and the mercury and sodium reservoirs

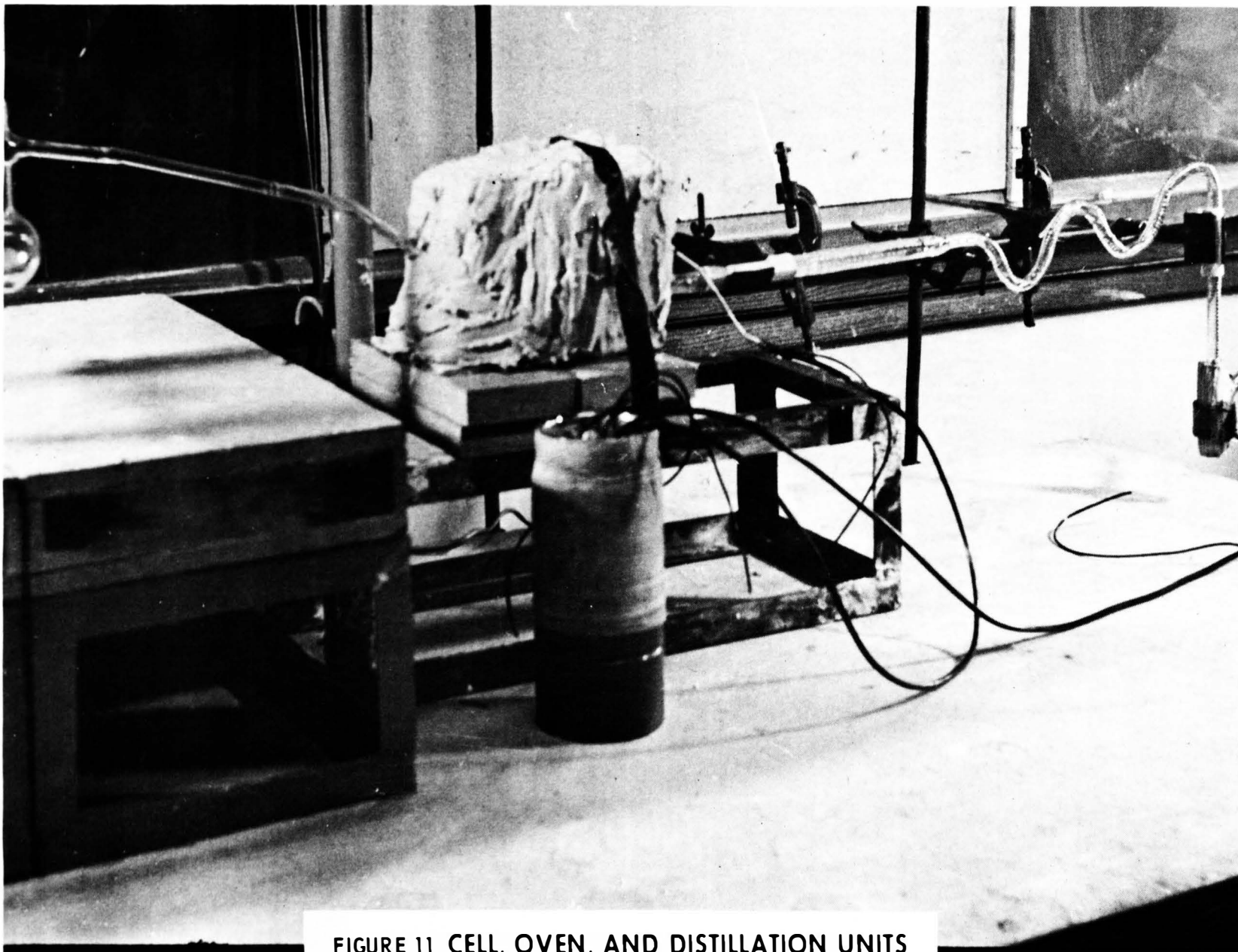


FIGURE 11 CELL, OVEN, AND DISTILLATION UNITS

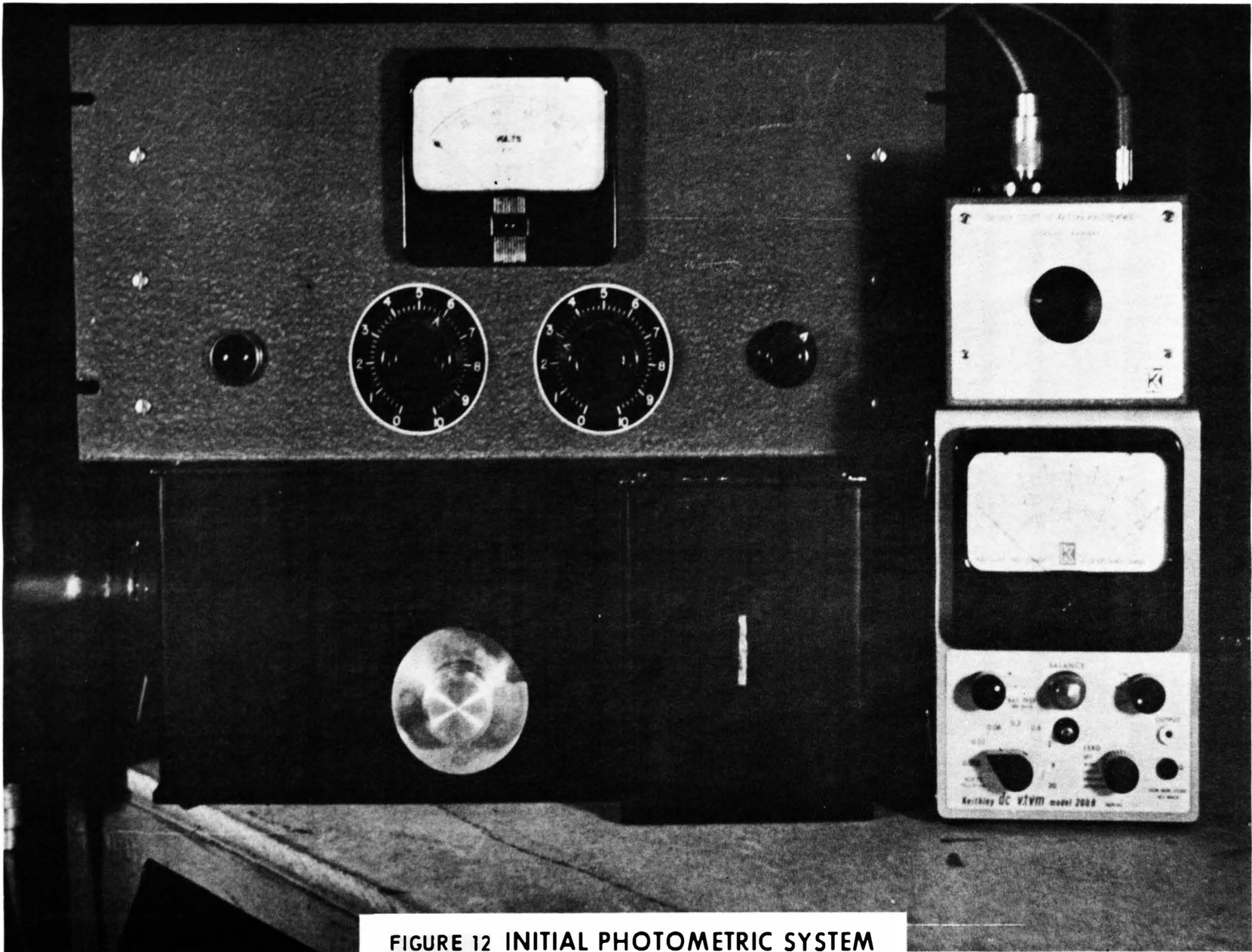


FIGURE 12 INITIAL PHOTOMETRIC SYSTEM

were mounted in separate ovens, so the vapor pressures of the two could be regulated by measuring their respective temperatures by means of thermocouples.

In the actual preparation of the absorption cell by the above method, the sodium was distilled into its reservoir and the distillation unit sealed off. In order to further clean up the sodium and its reservoir, the sodium reservoir oven was set at a moderate temperature and left to bake overnight. Upon returning in the morning it was discovered that the pressure in the system had gone to atmospheric pressure. Upon further investigation it was discovered that the sodium had reacted with the quartz, turning it a dark brown and literally disintegrating the sodium reservoir. Apparently, the sodium leached the oxygen from the crystal structure of the quartz and the resulting compound was a chalky, porous substance which disintegrated under the stresses produced by the atmospheric pressure outside the cell.

It was then early in June, 1960, and the author had accepted employment at McDonnell Aircraft Corporation. The system was contaminated and to rebuild the apparatus and run the experiment was an impossible task in the remaining time. So it was decided to leave and either return when the opportunity arose or try to finish the experiment at McDonnell.

In order to avoid the corrosion problems, the next attempt was to fabricate a cell of stainless steel with sapphire windows brazed to Kovar using the "active alloy process." The "active alloy process" together with other ceramic-to-metal bonds are described in Chapter 14 of Materials and Techniques for Electron Tubes¹¹. The process employed is as follows:

The sapphire window is painted with titanium hydride in the region where the seal is to be made. The brazing material is then placed between the titanium hydride and the metal part to which the window is to be brazed. As the unit is vacuum fired, the titanium hydride decomposes at around 900°C and leaves a film of titanium on the sapphire surface. As the temperature is slowly increased, the titanium diffuses into the sapphire and leaves a metallized surface which the braze can wet. The temperature is raised further until finally the braze melts and produces a vacuum joint between the Kovar and sapphire. Since the more common brazing alloys have one of the noble metals as their chief constituent, they cannot be used because they corrode in the presence of sodium and mercury. The alloy finally selected was a nickel, boron, silicon, manganese alloy tested by G. M. Slaughter et al¹².

However, before a successful sapphire-to-metal seal was fabricated, the process for sealing sapphire to Corning 7280, an alkali resistant glass, had been developed

at the Missouri School of Mines and Metallurgy. Since the major portion of the work on the metal cell had been completed, it was decided to use this cell to study a different system, and other people would work with the mercury-sodium system using a cell fabricated from Corning 7280 glass with a sapphire window. The cesium-rubidium system was chosen since the temperatures involved were not as high and hence the corrosion problem was reduced. Since the wavelengths involved were in the visible and near infra-red, it was also possible to use pyrex windows sealed to commercially available pyrex-to-Kovar tubular seals.

Final Apparatus

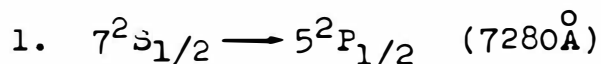
The second experimental apparatus was an all metal system and consisted of the following:

1. 2" CVC air cooled diffusion pump with a pumping speed of 25 liters/sec;
2. Welch mechanical pump model 91705;
3. Veeco ion gauge model RG-75 and Veeco electronic circuit model RG-21A;
4. liquid nitrogen cold trap;
5. stainless steel cell with pyrex windows;
6. Bristol 12 channel temperature recorder;
7. Osram 65 watt helium lamp model 50,056.

The entire system was constructed of 321 stainless steel, and all joints were heli-arc welded except the ion

gauge and window seals. Figure 13 shows the entire system with the cell mounted in the main oven. The cell was isolated from the pumping system with a Veeco stainless steel valve with a teflon seal. Figures 14 and 15 show the cell with the two reservoirs. The rubidium reservoir was maintained at the cell temperature and the cesium reservoir had a separate oven to control its temperature. The cesium and rubidium specimens were sealed in pyrex capsules after being distilled from their original capsules and they were inserted into the tubular metal appendages which can be seen in Figure 14. The front section of the cell, Figure 16, was then bolted on with a copper gasket used as the seal material. The system was then pumped down and baked at a temperature of 400°C for twelve hours. After cool down the system pressure was recorded at 3.3×10^{-7} Torr. The cesium and rubidium were introduced into the cell by crushing the glass capsules. The all metal cell was left attached to the vacuum system and the valve was used to isolate the cell.

The experiment was then set up and run with the spectrograph adjusted to detect light in the region from 6850\AA to 8230\AA , which covered seven of the transitions of interest. The following are the rubidium transitions and their corresponding wavelengths which were expected to occur in this region:



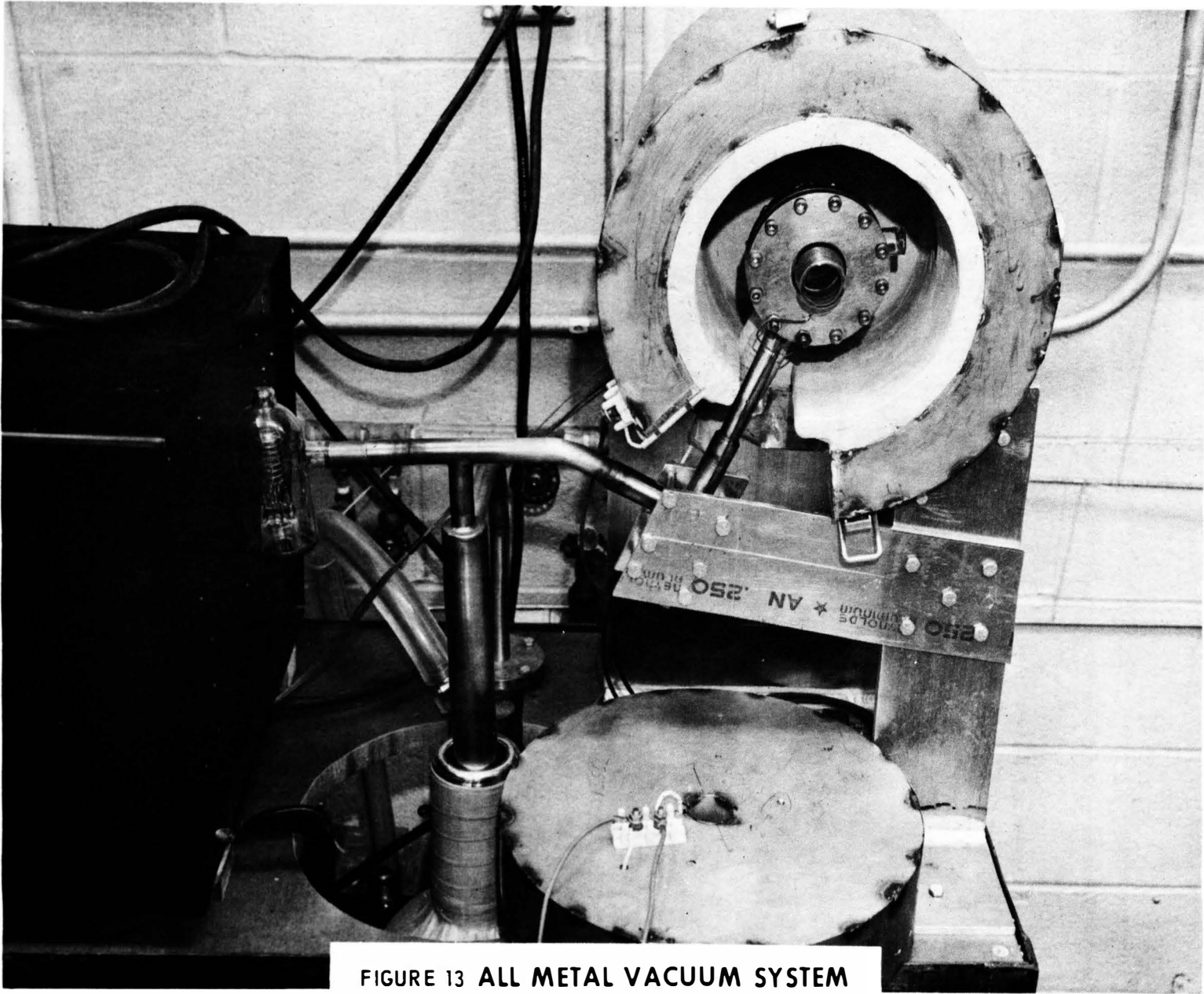


FIGURE 13 ALL METAL VACUUM SYSTEM

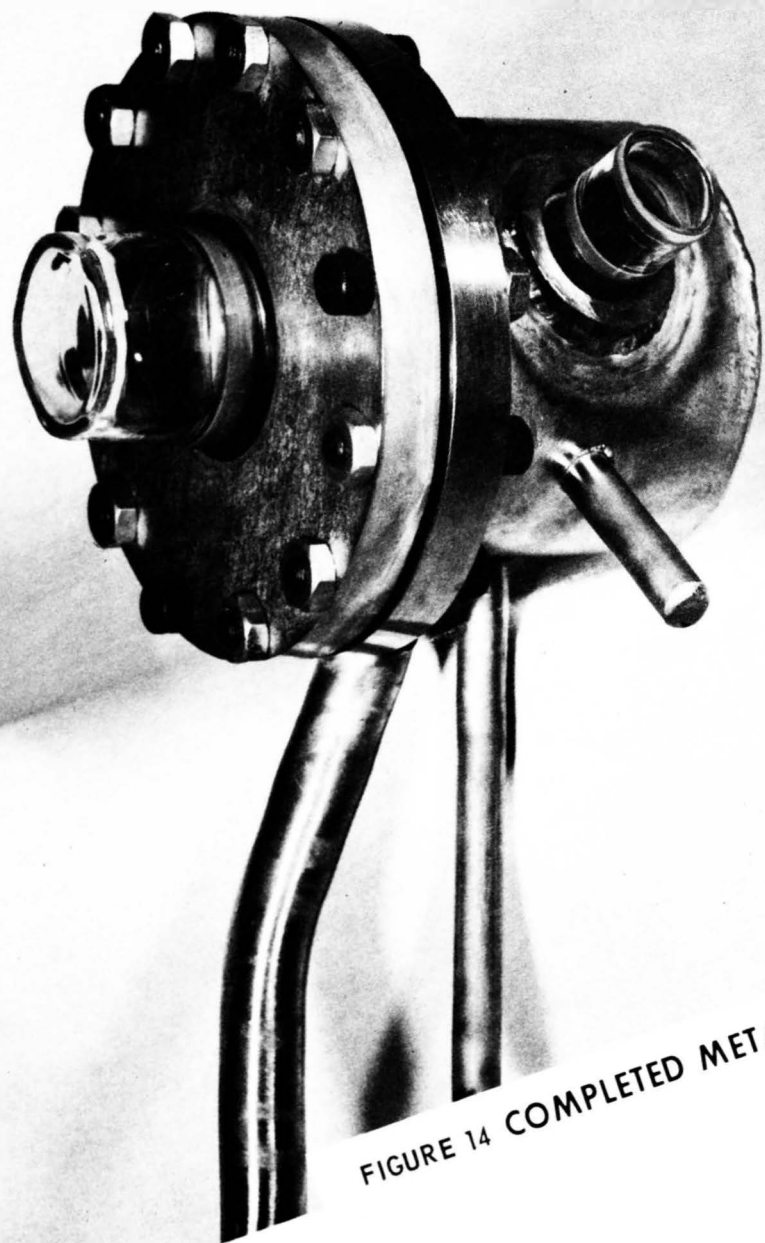


FIGURE 14 COMPLETED METAL CELL

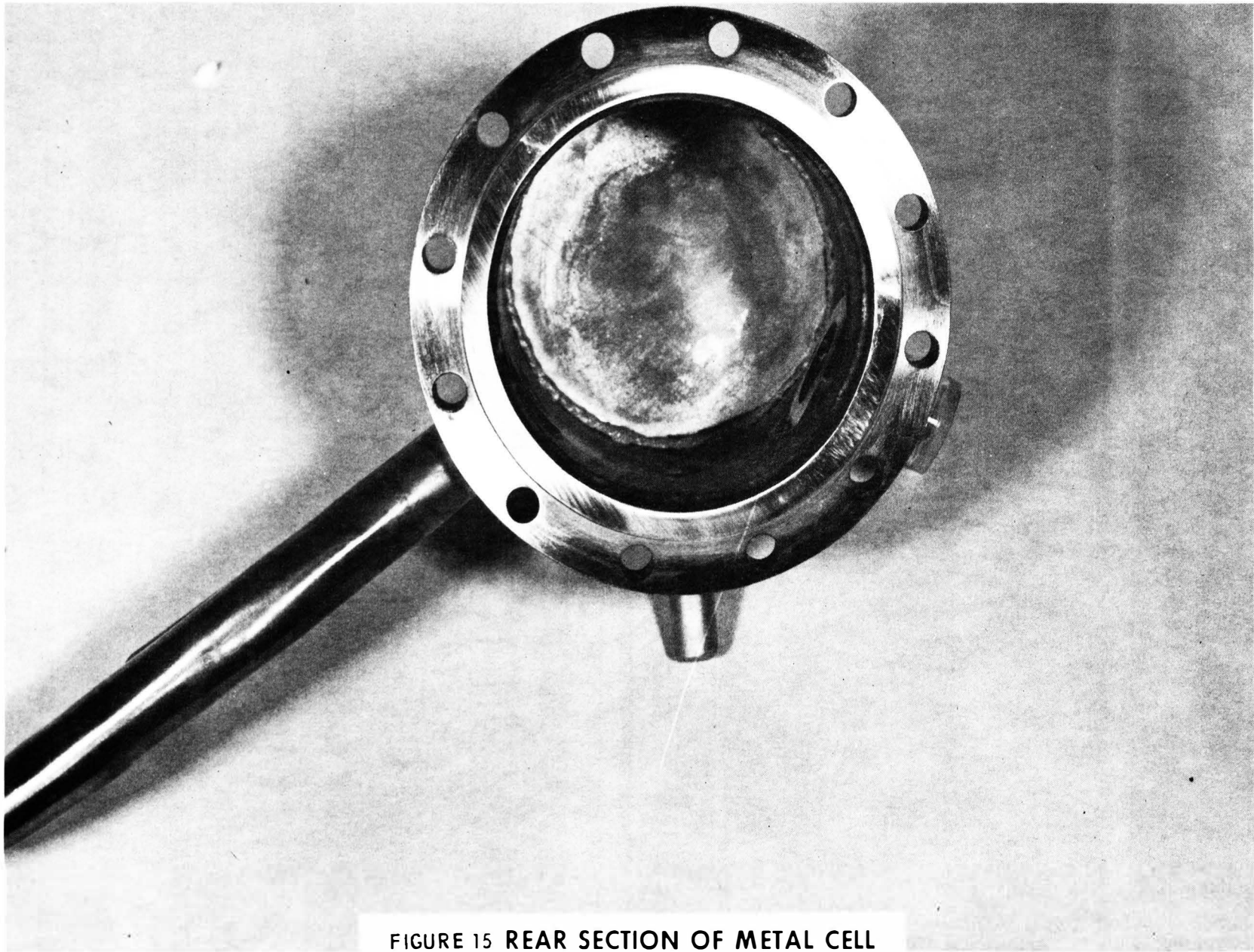


FIGURE 15 REAR SECTION OF METAL CELL

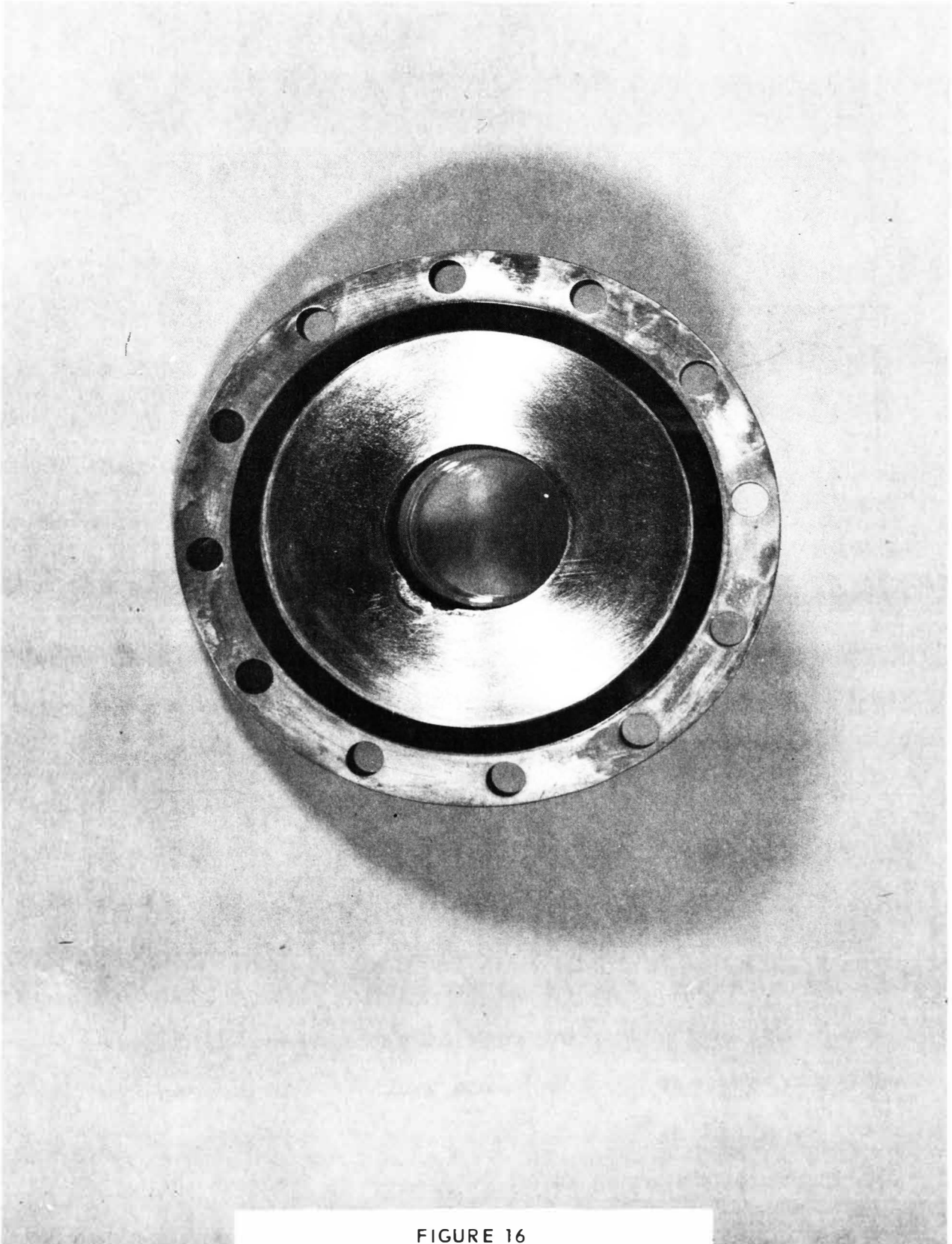


FIGURE 16
FRONT SECTION OF METAL CELL

2. $7^2S_{1/2} \rightarrow 5^2P_{3/2}$ (7408Å)
3. $5^2D_{3/2} \rightarrow 5^2P_{1/2}$ (7619Å)
4. $5^2D_{5/2} \rightarrow 5^2P_{3/2}$ (7758Å)
5. $5^2D_{3/2} \rightarrow 5^2P_{3/2}$ (7760Å)
6. $5^2P_{3/2} \rightarrow 5^2S_{1/2}$ (7800Å)
7. $5^2P_{1/2} \rightarrow 5^2S_{1/2}$ (7948Å)

Transitions 6 and 7 would appear only as cascade transitions from higher excited states and are of interest only because of this fact.

Four photographs were taken with each plate containing eight exposures. Tables I, II, III, and IV show the temperatures of the cesium and rubidium reservoirs during each exposure. Figures 17 and 18 are the vapor pressure curves for cesium and rubidium, respectively. In all cases the temperature represents the average of a continuous plot of the thermocouple output from a multichannel recorder. All system variables, such as power input to the ovens, excitation output of the lamp, and development procedure of the plates, were kept as constant as possible. After the plates were developed and inspected, there were no line spectra visible. After due consideration it was decided that either the transition probabilities were so small that the lines were not detectable or that some part of the testing procedure was in error. Since this experimental apparatus was designed to study the temperature dependence of the sensitized fluorescence, it was quite complex. It was therefore

TABLE I		
Photographic plate I-3 of sensitized fluorescence		
Exposure Time (Min.)	Cesium Temperature ($^{\circ}\text{C}$)	Rubidium Temperature ($^{\circ}\text{C}$)
1	142	145
3	141	145.5
5	141	145
7	141	145
9	142	146
11	143	147
13	143	147.5
15	143	148

TABLE II		
Photographic plate I-4 of sensitized fluorescence		
Exposure Time (Min.)	Cesium Temperature (°C)	Rubidium Temperature (°C)
1	216	202
3	216	202
5	216	202
7	216	202
9	216	203
11	216	204
13	216	204
15	217	204

TABLE III		
Photographic plate I-5 of sensitized fluorescence		
Exposure Time (Min.)	Cesium Temperature (°C)	Rubidium Temperature (°C)
1	312	274
3	312	274
5	312	276
7	309	276
9	311	276
11	311	277
13	312	277
15	312	277

TABLE IV		
Photographic plate I-6 of sensitized fluorescence		
Exposure Time (Min.)	Cesium Temperature ($^{\circ}\text{C}$)	Rubidium Temperature ($^{\circ}\text{C}$)
1	384	286
3	383	287
5	383	287
7	383	287
9	386	289
11	388	292
13	389	294
15	392	297

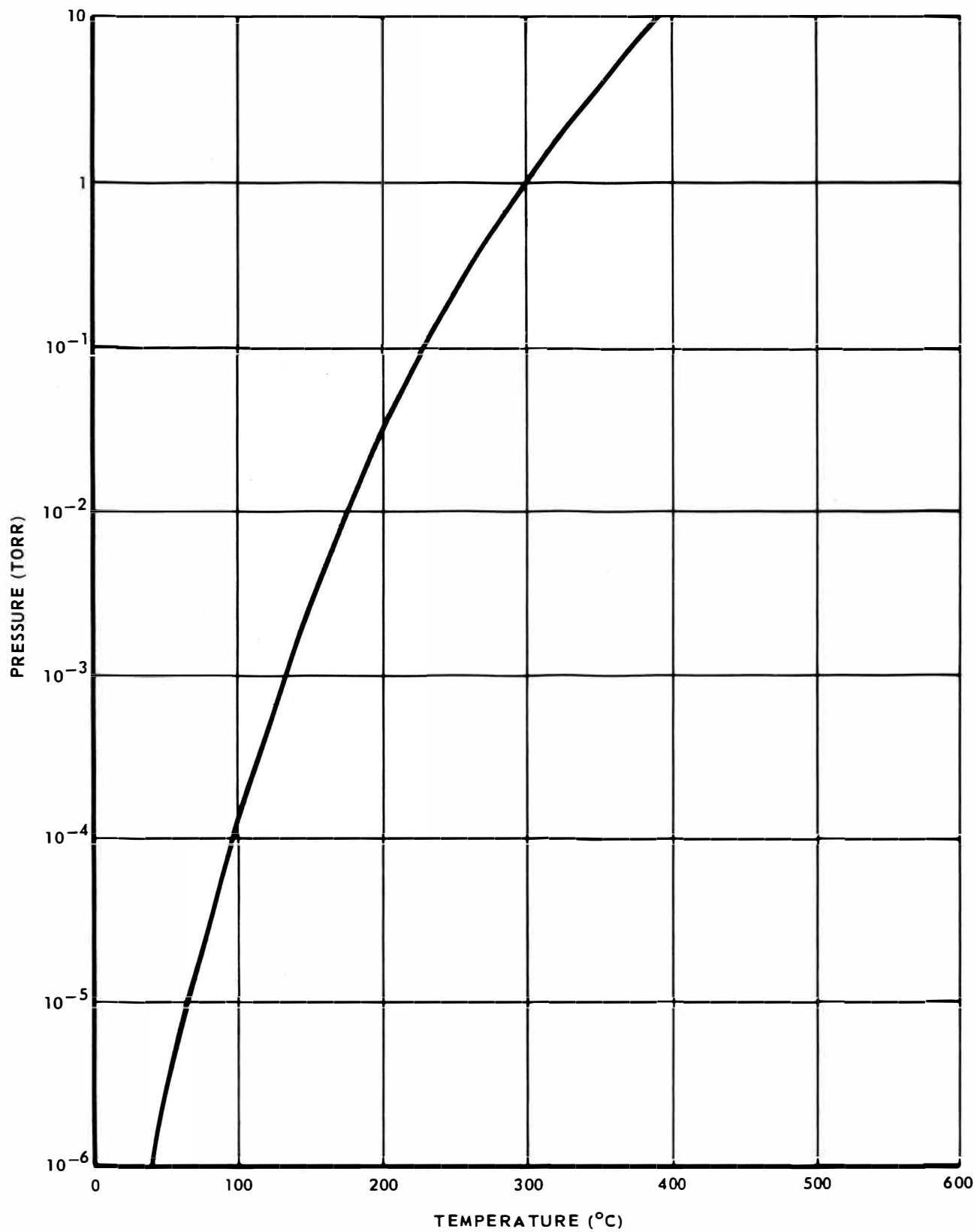


FIGURE 17
VAPOR PRESSURE CURVE FOR CESIUM

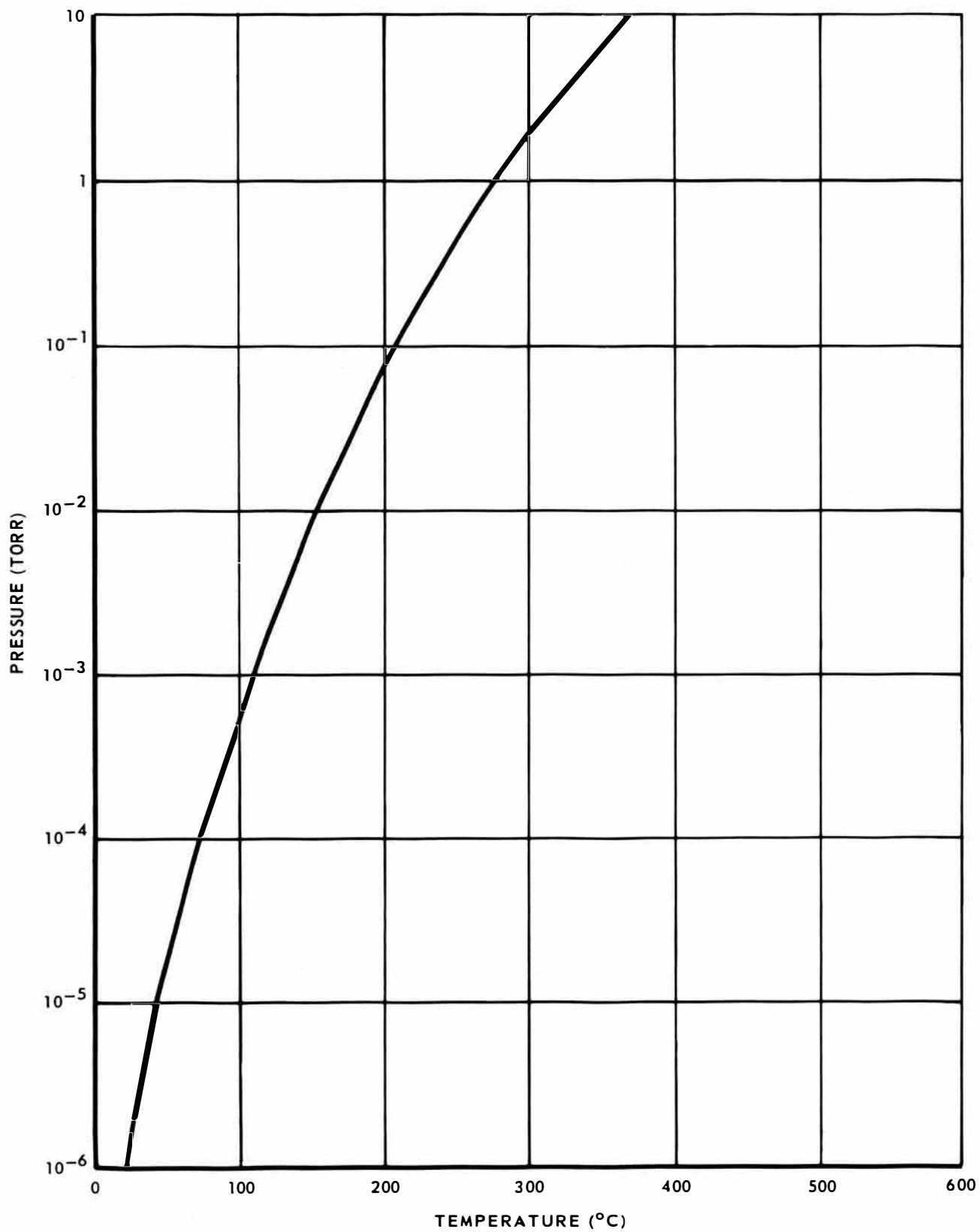


FIGURE 18
VAPOR PRESSURE CURVE FOR RUBIDIUM

decided that a simpler apparatus should be constructed to check for the possibility of an error in the test procedure or apparatus.

For a given temperature, the vapor pressure of cesium and rubidium are approximately the same. Therefore, after a short period of time, the two reservoirs contained a mixture of the two elements instead of a single element as is the case in most other experiments of this type. Therefore, no reservoirs were provided on the next cell and it was simply a cylindrical pyrex tube 3.5 inches long with pyrex windows on both ends. Figure 19 shows the completed cell with an approximate equal mixture of cesium and rubidium metal vacuum distilled into it. Figures 20 and 21 show the experimental apparatus with the cell mounted in the center of the oven. The main problem which was believed to have caused the negative results in the previous experiment was the difficulty of focusing the radiation emerging from the cell on the grating of the spectrograph. This was eliminated in the new apparatus, for the optical alignment could be checked by focusing the exciting radiation on the spectrograph and observing the incident light at the plateholder. Another series of exposures was taken at various temperatures and again no line spectra, except the incident helium lines, were visible after development of the plates. This time the oven temperature was held at 400°C for a long period of time and when the cell was removed from the



PYREX CYLINDRICAL CELL

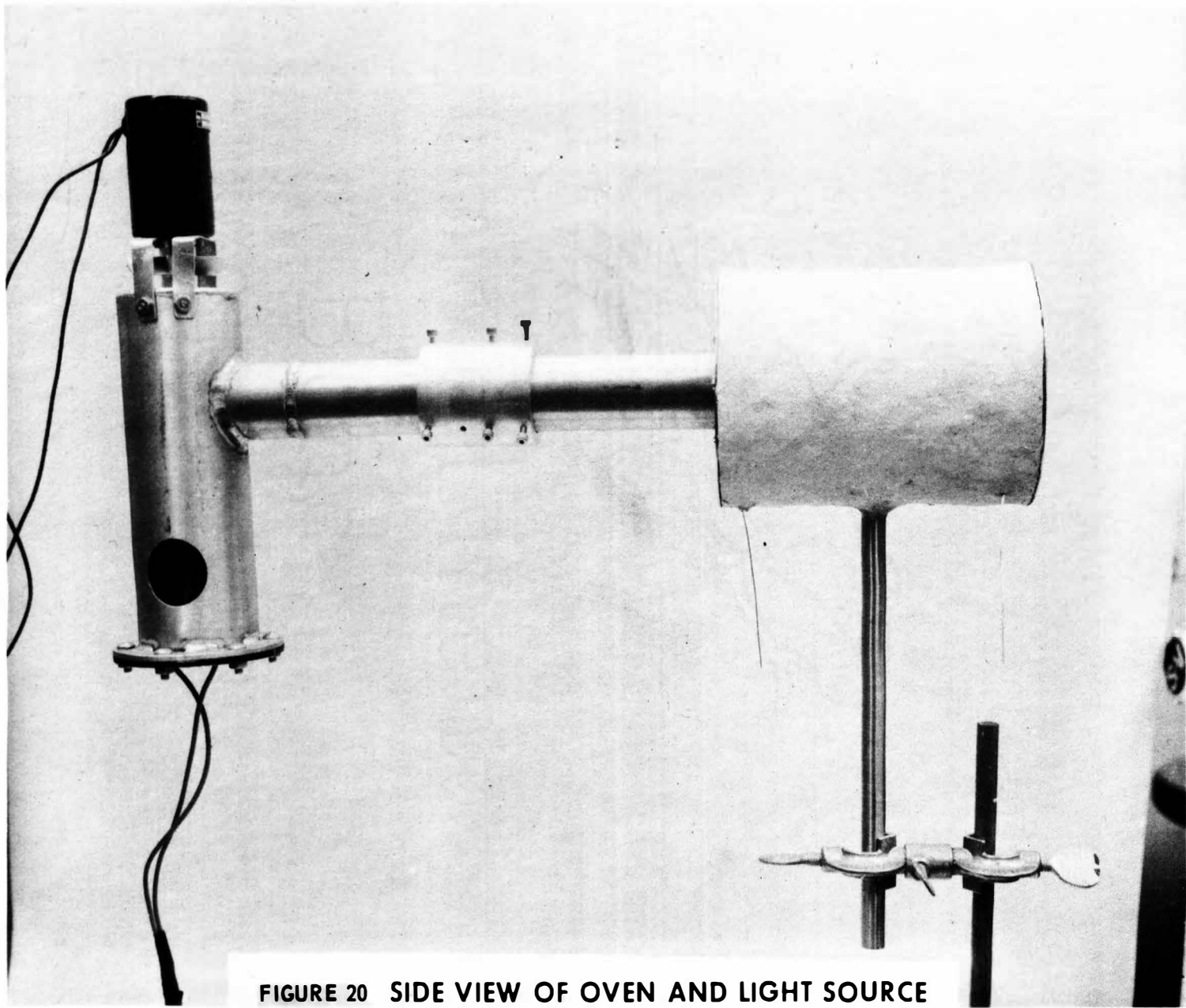


FIGURE 20 SIDE VIEW OF OVEN AND LIGHT SOURCE

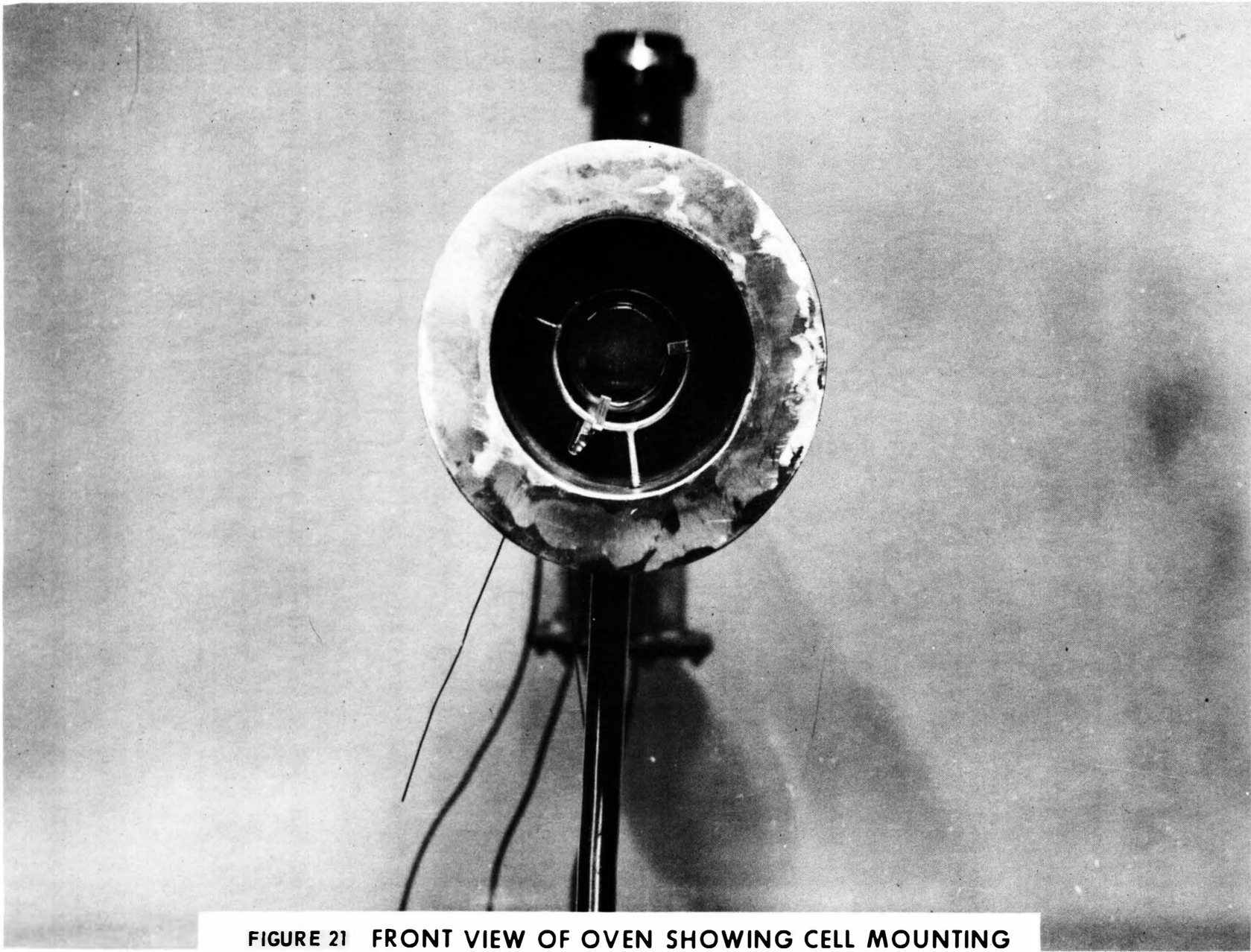


FIGURE 21 FRONT VIEW OF OVEN SHOWING CELL MOUNTING

oven, it was obvious that intergranular corrosion had taken place. Figures 22 and 23 show the cell after removal from the oven. It is not known at what point in the experiment this cell darkening took place, but from the fact that the pyrex windows of the cell in the previous test did not become darkened, it can be inferred that the corrosion was caused by extended exposure to the vapor at higher temperatures. Thus, data which was obtained at lower temperatures could be used.

At this point in the experiment it became apparent that possibly the transition probabilities were so low that the lines could not be detected. However, there still remained the task of obtaining data at the higher temperatures.

After consultation with Dr. Anderson, it was decided that a cell of Corning 7280 alkali resistant glass with sapphire windows should be constructed. The completed cell was similar to the pyrex cell shown in Figure 19 on page 50 and contained an approximate equal amount of vacuum distilled cesium and rubidium metal. However, during experimentation this cell cracked at the window seal and since it was not known when the damage took place, all the data had to be discarded for fear that gas leakage might have caused quenching of the lines if they had existed.

During this series of experiments it was decided that excitation at the rear window and detection at the front window might be in fault. There was danger that the



SIDE VIEW OF CORRODED PYREX CELL

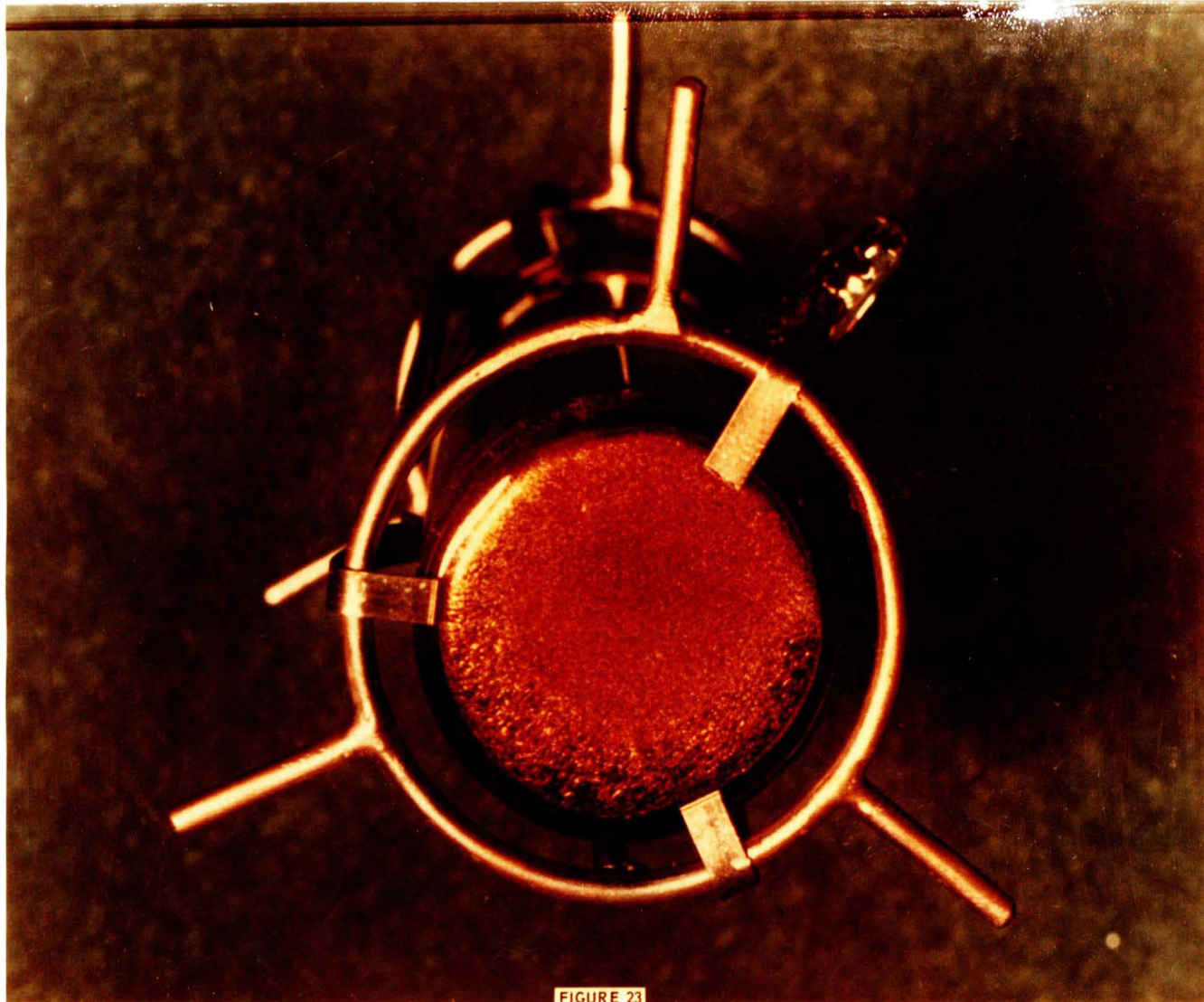


FIGURE 23

FRONT VIEW OF CORRODED PYREX CELL

incident radiation was absorbed by the cesium atoms in a thin cylindrical section at the rear of the absorption cell and there was no excitation of either cesium or rubidium over the full length of the absorption cell. This would result in a loss of output radiation of both cesium and rubidium lines if they were observed at the opposite end of the cell. In order to overcome this possible error, in the next series of data the vapor was excited by radiation incident on the front window and the emerging fluorescence was detected at the same window. Since only one window was needed, the next cell was fabricated from a cylindrical tube of Corning 7280 glass with only one sapphire end window. Figures 24, 25, and 26 show the test setup.

Since the suspicion of a negative result was growing stronger, in this last experiment rather than looking only for rubidium lines, possible cesium lines were also investigated. The following transitions and their corresponding wavelengths were investigated:

1. Rubidium $7^2S_{1/2} \rightarrow 5^2P_{1/2}$ (7280 $\overset{\circ}{\text{A}}$)
2. Rubidium $7^2S_{1/2} \rightarrow 5^2P_{3/2}$ (7408 $\overset{\circ}{\text{A}}$)
3. Rubidium $5^2D_{3/2} \rightarrow 5^2P_{1/2}$ (7619 $\overset{\circ}{\text{A}}$)
4. Rubidium $5^2D_{5/2} \rightarrow 5^2P_{3/2}$ (7758 $\overset{\circ}{\text{A}}$)
5. Rubidium $5^2D_{3/2} \rightarrow 5^2P_{3/2}$ (7760 $\overset{\circ}{\text{A}}$)
6. Rubidium $5^2P_{3/2} \rightarrow 5^2S_{1/2}$ (7800 $\overset{\circ}{\text{A}}$)
7. Rubidium $5^2P_{1/2} \rightarrow 5^2S_{1/2}$ (7948 $\overset{\circ}{\text{A}}$)
8. Rubidium $6^2P_{1/2} \rightarrow 5^2S_{1/2}$ (4216 $\overset{\circ}{\text{A}}$)

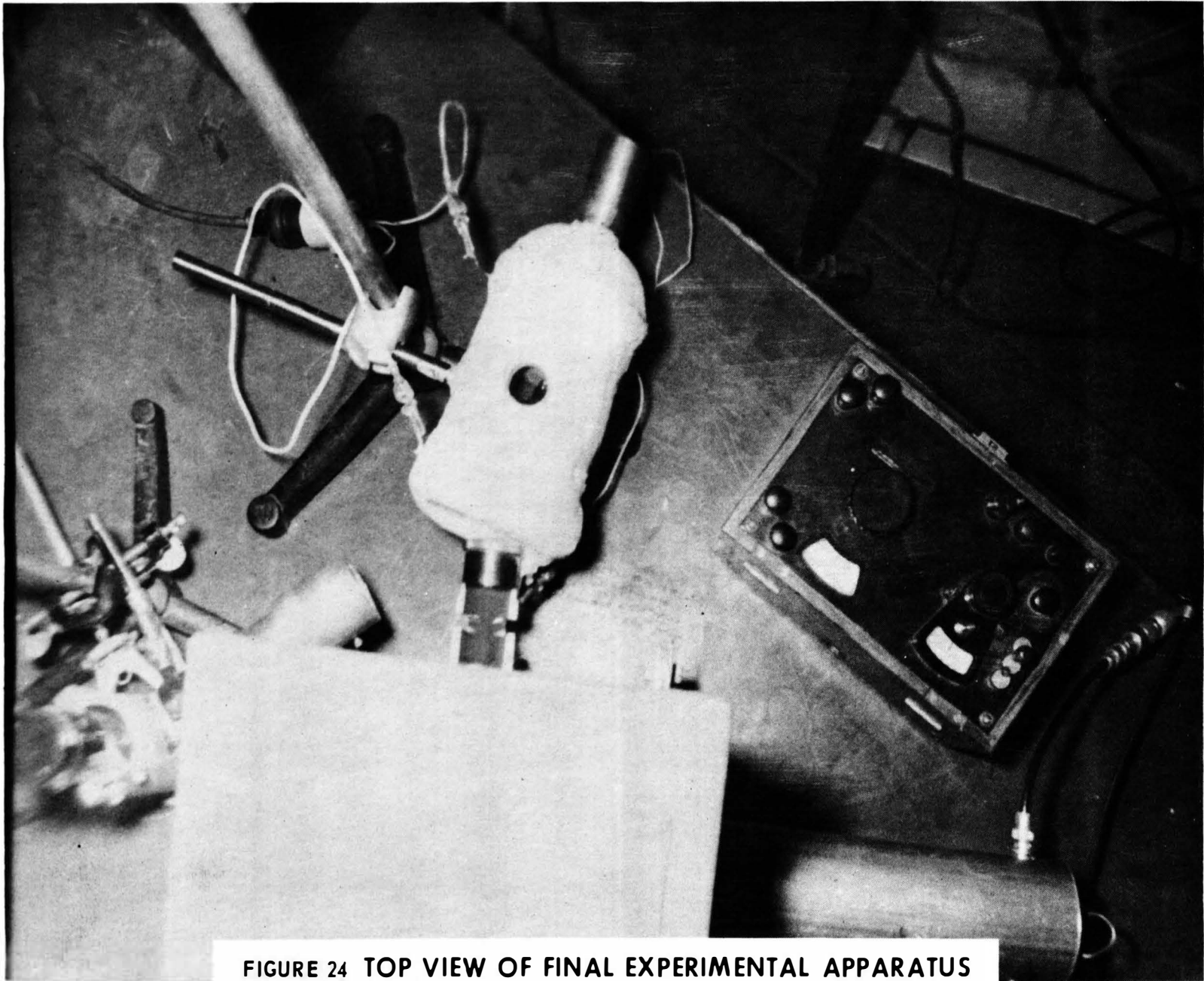


FIGURE 24 TOP VIEW OF FINAL EXPERIMENTAL APPARATUS

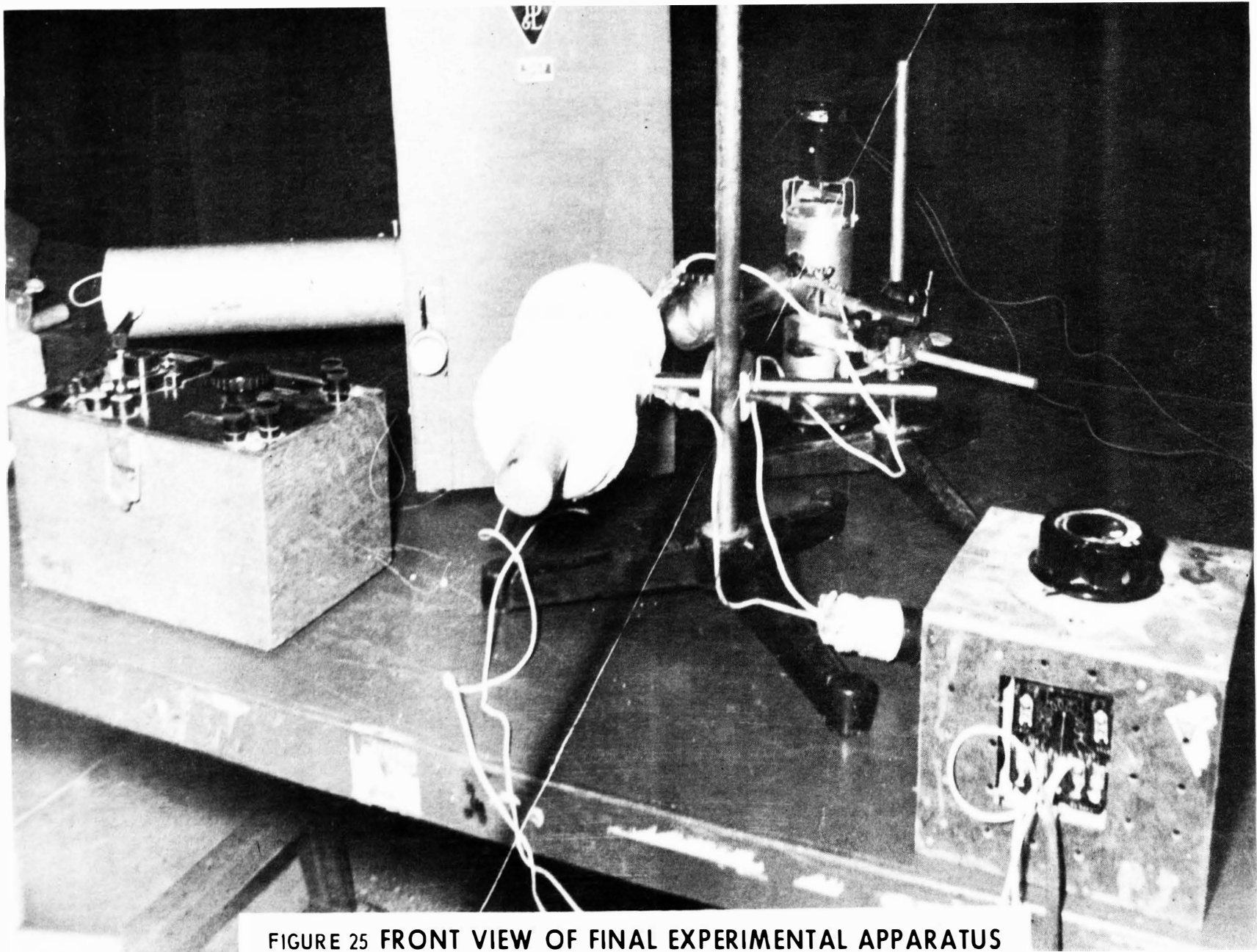


FIGURE 25 FRONT VIEW OF FINAL EXPERIMENTAL APPARATUS

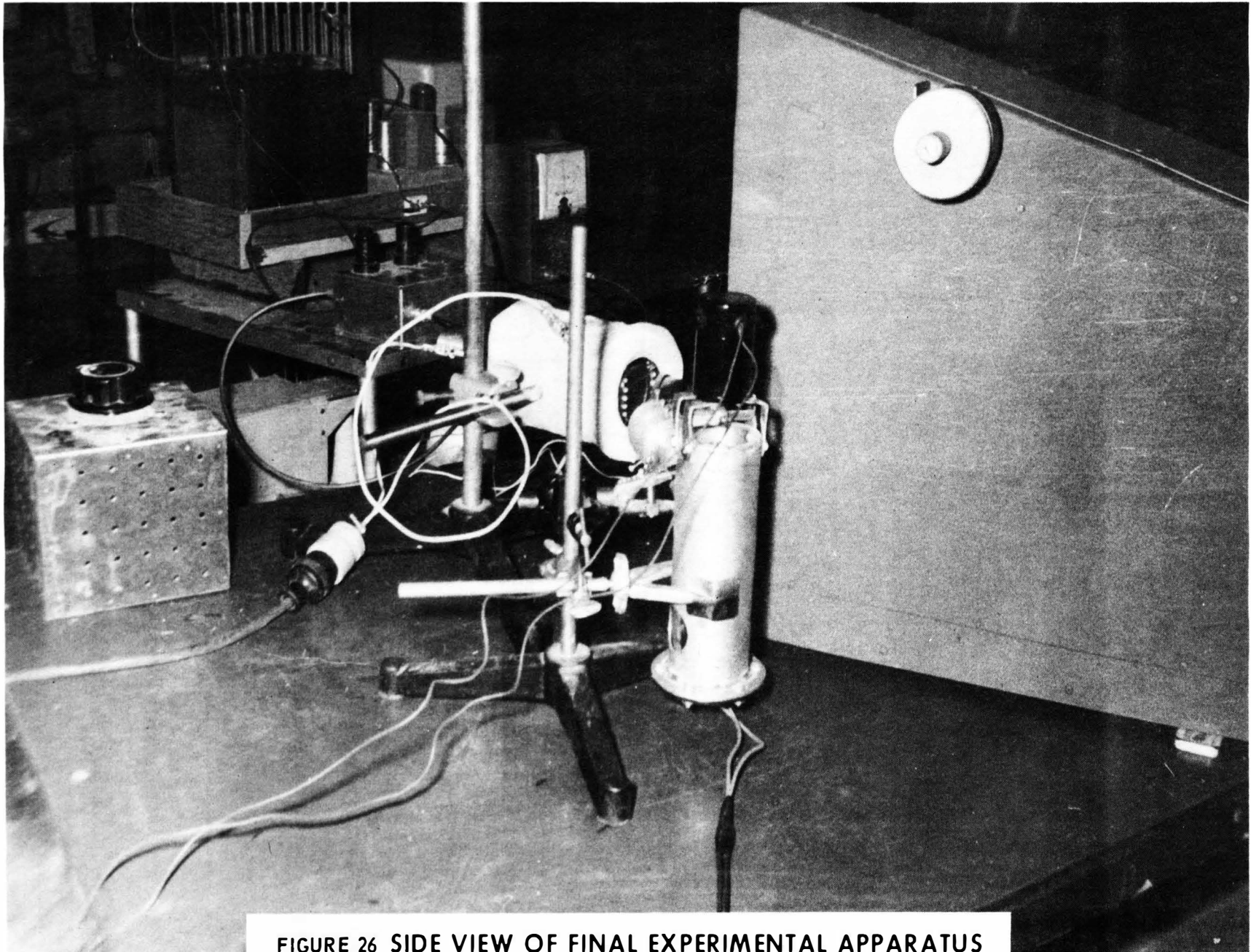


FIGURE 26 SIDE VIEW OF FINAL EXPERIMENTAL APPARATUS

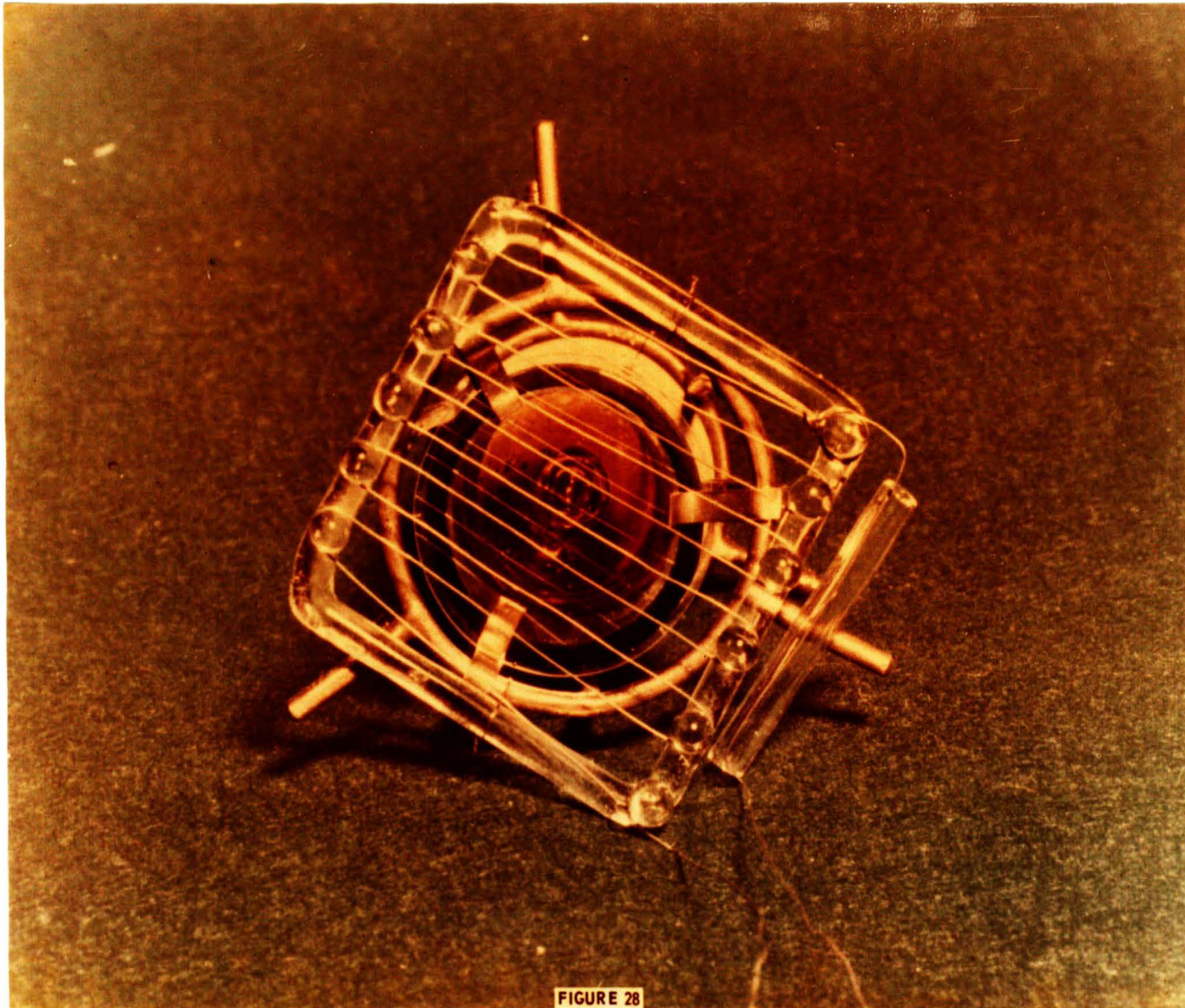
9.	Rubidium	$6^2P_{3/2} \rightarrow 5^2S_{1/2}$	(4202Å)
10.	Cesium	$8^2P_{3/2} \rightarrow 6^2S_{1/2}$	(3876Å)
11.	Cesium	$8^2S_{1/2} \rightarrow 6^2P_{3/2}$	(7946Å)
12.	Cesium	$8^2S_{1/2} \rightarrow 6^2P_{1/2}$	(7610Å)
13.	Cesium	$8^2P_{1/2} \rightarrow 5^2D_{3/2}$	(8921Å)
14.	Cesium	$6^2P_{1/2} \rightarrow 6^2S_{1/2}$	(8943Å)
15.	Cesium	$6^2P_{3/2} \rightarrow 6^2S_{1/2}$	(8522Å)

The oven temperature was varied so that vapor pressures of cesium from 8×10^{-2} Torr to 50 Torr and of rubidium from 3×10^{-2} Torr to 30 Torr existed in the cell. An RCA model 7102 electron multiplier, a twin-t amplifier, and an audio VTVM were used as the detection system. None of the lines of interest were detected. After removal of the cell for inspection, no damage other than a slight darkening of the Corning 7280 glass was apparent. The sapphire window remained clear even though temperatures up to 450°C were used. Figures 27 and 28 show the cell after removal from the oven.

The fact that the expected cesium transitions were not detectable could be explained in either of two ways. Either the cesium and rubidium together formed a quasi-molecule or stable compound for which the emission spectra is entirely different, or the amount of cesium excitation by the helium radiation was so small that it was undetectable or did not take place. The former seemed the more feasible of the two conclusions since there was experimental evidence for the



SIDE VIEW OF CORNING 7280 GLASS CELL



FRONT VIEW OF CORNING 7280 GLASS CELL

excitation of cesium vapor employing a helium source.

In order to resolve this dilemma, a cylindrical pyrex cell with one end window was fabricated and a small amount of cesium metal was vacuum distilled into it. Experiments were then performed to see if the expected cesium transitions occurred. The results were negative, which showed that the light source was not intense enough to produce a detectable amount of excitation of the cesium vapor.

V. DISCUSSION OF RESULTS AND CONCLUSIONS

Although no actual experimental data as such was obtained from this effort, much insight was obtained which could be applied to the design of a working system. These comments refer to the cesium-rubidium system. It has been proved that a cell constructed of Corning 7280 glass with sapphire windows will withstand temperatures up to 450°C in continuous operation. There is some discoloring of the 7280 glass, but no actual harm is done either to the glass or the sapphire which would be detrimental to the results. The only obvious error was in choosing a helium light source which was too weak to produce a detectable amount of cesium excitation. Perhaps this problem could be solved by using longer exposure times in the photographic method or by cooling the electron multiplier tube in the photometric method in order to decrease the background current. In order to insure results, either of these modifications plus a more intense light source should be employed. It is recommended that two high pressure helium arc sources be used as straight tubes at the focal point of a cylindrical parabolic or elliptic reflector or a high pressure helical spiral helium source be used which surrounds the cell. In either arrangement, there should be specimen reservoirs external to the main cell oven so the vapor pressures of both metals can be controlled and measured.

The cell and associated vacuum system could be constructed either of glass or metal, whichever is preferred. If the system is constructed of glass, pyrex can be used wherever parts which are exposed to cesium or rubidium vapor do not exceed 350°C . Since this limits the versatility of the cell, it should be constructed of Corning 7280 glass with sapphire end windows for use above this temperature. A metal system could be employed, fabricated of weldable stainless steel. The preferred material is a 300 series stainless with joints being heli-arc welded. Any braze joints which are used must employ an alloy containing none of the precious metals in regions exposed for any length of time to cesium or rubidium vapor at elevated temperatures.

Either of the detection systems, photographic or photometric, are adequate and exhibit enough sensitivity to successfully run the experiment. Both systems were able to detect the majority of the helium lines in the region of interest and could give relative intensity measurements. If the light source problem were improved, an extensive study of the properties of the sensitized fluorescence of the cesium-rubidium system could be performed.

BIBLIOGRAPHY

1. O. Klein and S. Rosseland, Z. f. Phys. 4, 46(1921).
2. H. Beutler and B. Josephy, Z. f. Phys. 53, 747(1929).
3. R. Swanson and R. McFarland, Phys. Rev. 98, 1063(1955).
4. J. Winans, Rev. Mod. Phys. 16, 175(1944).
5. C. Boeckner, B. S. Jour. Research 5, 13(1930).
6. F. L. Mohler and C. Boeckner, B. S. Jour. Research 5, 399(1930).
7. S. Jacobs, G. Gould, and P. Rabinowitz, Phys. Rev. Letters 7, 415(1961).
8. J. R. Singer (ed.), Advances in Quantum Electronics (Columbia University Press, New York and London, 1961).
9. R. A. Anderson and E. E. Stepp, Rev. Sci. Instr. 33, 119(1962).
10. Ralph A. Sawyer, Experimental Spectroscopy (Dover Publications, Inc., New York, 1963).
11. Walter H. Kohl, Materials and Techniques for Electron Tubes (Reinhold Publishing Corp., New York, Chapman and Hall Ltd., London, 1960).
12. G. M. Slaughter et al., Welding Jour. 36, 217(1957).

VITA

The author was born in Montrose, Missouri, the son of Mr. and Mrs. Edward J. Hueser, on June 6, 1937. He attended grade school and high school in Kansas City, Missouri. He entered Rockhurst College in Kansas City, Missouri, in September of 1954 and received a Bachelor of Science degree in Physics in June, 1958. Graduate study at the University of Missouri, School of Mines and Metallurgy, was begun in September, 1958. From June, 1960, until the present time he has worked at McDonnell Aircraft Corporation in St. Louis, Missouri, in the Physics Laboratory.